Exotic hadrons in heavy ion collisions

Sungtae Cho,[1] Takenori Furumoto,[2,3] Tetsuo Hyodo,[4] Daisuke Jido,[2] Che Ming Ko,[5] Su Houng Lee,[1] Marina Nielsen,[6]
Akira Ohnishi,[2] Takayasu Sekihara,[2,7] Shigehiro Yasui,[8] and Koichi Yazaki[2,9]

(ExHIC Collaboration)

[1]*Institute of Physics and Applied Physics, Yonsei University, Seoul 120-749, Korea*
[2]*Yukawa Institute for Theoretical Physics, Kyoto University, Kyoto 606-8502, Japan*
[3]*RIKEN Nishina Center, Hirosawa 2-1, Wako, Saitama 351-0198, Japan*
[4]*Department of Physics, Tokyo Institute of Technology, Meguro 152-8551, Japan*
[5]*Cyclotron Institute and Department of Physics and Astronomy, Texas A&M University, College Station, Texas 77843, USA*
[6]*Instituto de Física, Universidade de São Paulo, C.P. 66318, 05389-970 São Paulo, São Paulo, Brazil*
[7]*Department of Physics, Graduate School of Science, Kyoto University, Kyoto 606-8502, Japan*
[8]*Institute of Particle and Nuclear Studies, High Energy Accelerator Research Organization (KEK), 1-1, Oho, Ibaraki 305-0801, Japan*
[9]*Hashimoto Mathematical Physics Laboratory, Nishina Center, RIKEN, 2-1, Hirosawa, Wako, Saitama 351-0198, Japan*

We investigate the possibilities of using measurements in present and future experiments on heavy ion collisions to answer some longstanding problems in hadronic physics, namely, identifying hadronic molecular states and exotic hadrons with multiquark components. The yields of a selected set of exotic hadron candidates in relativistic heavy ion collisions are discussed in the coalescence model in comparison with the statistical model. We find that the yield of a hadron is typically an order of magnitude smaller when it is a compact multiquark state, compared to that of an excited hadronic state with normal quark numbers. We also find that some loosely bound hadronic molecules are formed more abundantly than the statistical model prediction by a factor of two or more. Moreover, owing to the significant numbers of charm and bottom quarks produced at RHIC and even larger numbers expected at LHC, some of the proposed heavy exotic hadrons could be produced with sufficient abundance for detection, making it possible to study these new exotic hadrons in heavy ion collisions.

I. INTRODUCTION

Experiments at the Relativistic Heavy Ion Collider (RHIC) during the past decade have shown that the properties of the quark-gluon plasma (QGP) formed in heavy ion collisions are far more intriguing than originally conceived [1]. Instead of weakly interacting, the QGP was found to be a strongly coupled system with so small a shear viscosity that it behaves like an ideal fluid. The study of the QGP is expected to remain an active field of research in the future because of the proposed upgrade of RHIC and new experimental possibilities at the Large Hadron Collider (LHC). The physics of QGP is related to a wide range of other fields, such as the early universe, nonequilibrium statistical physics, string theory by AdS/CFT correspondence, and so on.

During the same time, there have also been exciting developments in the spectroscopy of heavy hadrons, starting with the discovery of the $D_{sJ}(2317)$ by the BABAR Collaboration [2], whose mass could not be explained by the simple quark model, and the $X(3872)$ by the Belle Collaboration [3], whose mass and decay channel strongly support a nontrivial fraction of $\bar{D}D^*$ and $D\bar{D}^*$ components in its wave function. The Belle collaboration also reported the finding of the $Z^+(4430)$ in the $\psi'\pi^+$ spectrum [4]. Because the $Z^+(4430)$ is a charged state, it cannot be a simple $c\bar{c}$ state. If confirmed, this would be the first evidence for the existence of an exotic hadron that is composed of two quarks and two antiquarks such as $c\bar{c}u\bar{d}$ [5,6].

The question of whether multiquark hadrons exist is an old problem in the light hadron sector that began with

attempts to understand the inverted mass spectrum of the scalar nonet [$a_0(980)$, $f_0(980)$, and so on] in the tetraquark picture [7,8]. Also, the exotic H dibaryon was proposed on the basis of the color-spin interaction [9], and it has been sought for in various experiments for a long time without success. On the other hand, the $\Lambda(1405)$ baryon resonance was considered as a $\bar{K}N$ quasibound state in the $\bar{K}N - \pi\Sigma$ coupled-channel analysis [10]. With further development of the coupled-channel approach [11], it has been realized that the $\Lambda(1405)$ is the most obvious and uncontroversial candidate for a hadronic molecule, whose wave function is composed dominantly of a $\bar{K}N$ bound state mixed with a small $\pi\Sigma$ resonant state [12]. If such a configuration for the $\Lambda(1405)$ is confirmed in experimental measurements, it will be the first evidence for a molecular hadronic state. Many new multiquark states such as $\bar{K}KN$, $\bar{K}NN$, $(\Omega\Omega)_0$, etc., have also been predicted.

While the $Z^+(4430)$ could be the first explicitly exotic hadron found to date, it will be a milestone in hadronic spectroscopy if other flavor exotic hadrons are found, such as the controversial pentaquark $\Theta^+(udud\bar{s})$ first reported in experiments on photonuclear reactions [13]. Also, several other flavor exotic molecular and compact multiquark hadrons were previously predicted, based, respectively, on the meson-exchange and color-spin interactions. More recently, a simple diquark model based on the color-spin interaction [14,15] was shown to naturally explain the likely existence of flavor exotic multiquark hadrons consisting of heavy spectator quarks, such as the $T_{cc}^1(ud\bar{c}\bar{c})$, $T_{cb}^0(ud\bar{c}\bar{b})$, and $\Theta_{cs}(udus\bar{c})$

that were predicted before, and the newly predicted dibaryon $H_c^{++}(udusc)$. Furthermore, the stable molecular bound states $\bar{D}N$ and $\bar{D}NN$ in the charmed sector and the BN and BNN in the bottom sector have been predicted to exist as a result of the long-range pion-exchange potential [16,17].

To gain insights into all these proposals and questions [14,18,19], we have proposed in recent publications [20,21] a new approach of studying exotic hadrons in heavy ion collisions at ultrarelativistic energies. There are several merits for this approach compared to the search for exotic hadrons in elementary particle reactions that have been pursued so far. First, an appreciable number of heavy quarks are expected to be produced in these collisions, reaching as much as 20 $\bar{c}c$ pairs per unit rapidity in Pb + Pb collisions at the LHC [22]. Second, through vertex reconstruction of weakly decaying particles, one could substantially reduce the backgrounds in the detection, making the identification of weakly decaying exotics possible. Finally, because of the large volume of quark and hadronic matters formed in these collisions and the new paradigm of hadronization through coalescence [23–25], various exotic hadrons could be formed from the recombinations of quarks. We have therefore investigated in Refs. [20,21] the possibility of using measurements in present and future experiments on heavy ion collisions to answer the longstanding problems in hadronic physics of identifying and examining hadronic molecular states and exotic hadrons that consist of multiquarks.

In the present paper, we extend the discussions in Ref. [20] to include all exotic hadrons that have been proposed so far. These hadrons are classified as exotic mesons, exotic baryons, and exotic dibaryons, and for each exotic hadron we give a brief summary of its properties and the status on the latest researches. Moreover, we collect all necessary references so that the present paper can be used as a general guide to the literatures on exotic hadrons. Using this information, we then evaluate their yields in heavy ion collisions based on both the statistical and the coalescence model. In particular, we present a detailed description of the calculations carried out in Ref. [20] with an emphasis on the expected yields of exotic hadrons in heavy ion collisions at LHC.

The statistical model is based on the assumption that hadrons produced in relativistic heavy ion collisions are in thermal and chemical equilibrium at temperatures that are close to that for the QGP to hadronic matter phase transition, and it has been known to describe very well the relative yields of normal hadrons [26]. The coalescence model, on the other hand, describes hadron production through the coalescence or recombination of particles [23–25]. The model has successfully explained observed enhancement in the production of midrapidity baryons in the intermediate transverse momentum region [27,28], the quark number scaling of the elliptic flow of identified hadrons [29,30], and the yield of antihypertritons recently discovered in heavy ion collisions at RHIC [31]. Furthermore, the coalescence model that takes into account the internal structure of hadrons has been shown in Ref. [32] to be able to describe the observed suppression of the $\Lambda(1520)$ yield in heavy ion collisions at RHIC compared to the prediction of the statistical model [33]. As in Ref. [20], we fix the parameters in the coalescence model by reproducing the yields of normal

hadrons in the statistical model [26]. We then apply these two models to calculate the yields of exotic hadrons. As reference particles for the comparison with exotic hadrons, we consider, in particular, normal hadrons such as the strange $\Lambda(1115)$ and $\Lambda(1520)$, the charmed $\Lambda_c(2286)$, and the bottom $\Lambda_b(5620)$. Our results show that the yields of proposed exotic mesons, baryons, and dibaryons are large enough for carrying out realistic measurements. We further discuss their most probable weak decay channels that can be observed in experiments.

Our study shows that results from the coalescence model are sensitive to the inner structure of hadrons, such as the angular momentum, quark numbers and so on. This is different for the statistical model, because the yields of the hadrons in this model are determined mainly by their masses. To discriminate the different pictures for exotic hadrons, we can thus compare the results from the coalescence model with those from the statistical model. We find that the relative yields of light exotic hadrons in the coalescence model are very different from those in the statistical model, and this makes it possible to experimentally discriminate among the different pictures for their structures, such as multiquarks versus hadronic molecules.

This paper is organized as follows. In Sec. II, we describe briefly the schematic model used for describing the time evolution of the hot dense matter formed in relativistic heavy ion collisions. We then explain the statistical model and the coalescence model used in the present study. The properties of the exotic hadrons included in this work and their predicted yields are given in Secs. III and IV, respectively. This is followed by discussions in Sec. V and conclusions in Sec. VI. In Appendix A, we derive the Wigner function of hadrons whose structures are described by the d wave and the corresponding coalescence factor. We also give in Appendix B the coalescence factors for the general l-wave harmonic oscillator wave functions. In Appendix C, we discuss the effect from the width of resonances to the yields of the exotic hadrons both in the coalescence model and in the statistical model.

II. MODELS FOR HADRON PRODUCTION

A. Heavy ion collision dynamics

For the dynamics of central relativistic heavy ion collisions, we use the schematic model of Ref. [18] based on isentropic boost invariant longitudinal and accelerated transverse expansions. In this model, both the initial QGP and final hadronic matter are treated as noninteracting free gas, and the transition between these two phases of matter is taken to be first order. The time evolution of the temperature and volume of the system is determined by the entropy conservation. In Table I, we tabulate the values of the critical or hadronization temperature T_C and volume V_C at the beginning of the quark-gluon to hadronic matter phase transition, the volume V_H at the end of the mixed phase or hadronization, and the kinetic or thermal freeze-out temperature T_F and volume V_F for both central Au + Au collisions at $\sqrt{s_{NN}} = 200$ GeV at RHIC and central Pb + Pb collisions at $\sqrt{s_{NN}} = 5$ TeV at LHC. Also given in Table I is the abundance of various quarks at T_C.

TABLE I. Quark numbers at hadronization temperature T_C and volume V_C, the volume V_H at the end of hadronization, and the thermal freeze-out temperature T_F and volume V_F in central heavy ion collisions at RHIC and LHC.

	RHIC	LHC
$N_u = N_d$	245	662
$N_s = N_{\bar{s}}$	150	405
$N_c = N_{\bar{c}}$	3	20
$N_b = N_{\bar{b}}$	0.02	0.8
V_C	1000 fm^3	2700 fm^3
$T_C = T_H$	175 MeV	175 MeV
V_H	1908 fm^3	5152 fm^3
μ_B	20 MeV	0 MeV
μ_s	10 MeV	0 MeV
V_F	11322 fm^3	30569 fm^3
T_F	125 MeV	125 MeV

As described in the next sections, hadron production in the statistical model occurs in the volume V_H at the temperature T_H, which is assumed to be the same as T_C, while in the quark coalescence model, the production of both ordinary and multiquark hadrons occurs at the temperature T_C when the volume of the QGP is V_C. For the production of hadronic molecular states from the coalescence of hadrons, it takes place, however, in the volume V_F at the kinetic freeze-out temperature T_F.

B. The statistical model

The statistical model has been shown to describe very well the relative yields of normal hadrons in relativistic heavy ion collisions. In this model, the number of produced hadrons of a given type h is given by [26]

$$N_h^{\text{stat}} = V_H \frac{g_h}{2\pi^2} \int_0^\infty \frac{p^2 dp}{\gamma_h^{-1} e^{E_h/T_H} \pm 1} \quad (1)$$

$$\approx \frac{\gamma_h g_h V_H}{2\pi^2} m_h^2 T_H K_2(m_h/T_H) \quad (2)$$

$$\approx \gamma_h g_h V_H \left(\frac{m_h T_H}{2\pi}\right)^{3/2} e^{-m_i/T_H}, \quad (3)$$

In the above equations, g_h is the degeneracy of the hadron and γ_h is the fugacity, and V_H and T_H are, respectively, the volume and temperature of the source when statistical production occurs.

Because strangeness is known to reach approximate chemical equilibrium in heavy ion collisions at RHIC owing to the short equilibration time in the QGP and the net strangeness of the QGP is zero, the strange chemical potential is small and is taken to be $\mu_s = 10$ MeV. Its value decreases with increasing collision energy and is assumed to be 0 MeV in heavy ion collisions at LHC. For charm and bottom quarks, they are produced from initial hard scattering and their numbers are much larger than those expected from a chemically equilibrated QGP. As a result, we obtain the fugacity $\gamma_h > 1$ for both charmed and bottom hadrons. In terms of the fugacities γ_c and γ_b of charm and bottom quarks, the fugacities of charmed

and bottom hadrons are products of γ_c^n and γ_b^m, where n and m are, respectively, the charm and bottom quark numbers in these hadrons. Therefore, the fugacity of hadron species h can be written generally as

$$\gamma_h = \gamma_c^{n_c + n_{\bar{c}}} \gamma_b^{n_b + n_{\bar{b}}} e^{(\mu_B B + \mu_s S)/T_H}, \quad (4)$$

where B, S, n_c ($n_{\bar{c}}$), and n_b ($n_{\bar{b}}$) are the baryon number, strangeness, (anti-)charm quark number, and (anti-)bottom quark number of the hadron, respectively.

For the charm and bottom fugacities γ_c and γ_b, they can be determined by requiring that the total yield of charmed or bottom hadrons estimated in the statistical model is the same as the expected total charm (N_c) or bottom (N_b) quark number from initial hard nucleon-nucleon scattering. Using the values $N_c = 3$ and $N_b = 0.02$ for heavy ion collisions at RHIC, we obtain $\gamma_c = 6.40$ and $\gamma_b = 2.2 \times 10^6$ according to the following calculations:

$$N_c = N_D + N_{D^*} + \frac{1}{2}\left(N_{D_s} + N_{\bar{D}_s}\right) + \frac{1}{2}\left(N_{\Lambda_c} + N_{\bar{\Lambda}_c}\right)$$
$$= 1.04 + 1.53 + \frac{0.33 + 0.29}{2} + \frac{0.14 + 0.11}{2} = 3, \quad (5)$$

$$N_b = N_{\bar{B}} + N_{\bar{B}^*} + \frac{1}{2}\left(N_{\bar{B}_s} + N_{B_s}\right) + \frac{1}{2}\left(N_{\Lambda_b} + N_{\bar{\Lambda}_b}\right)$$
$$= 5.3 \times 10^{-3} + 1.23 \times 10^{-2}$$
$$+ \frac{1.7 + 1.5}{2} \times 10^{-3} + \frac{9.2 + 7.3}{2} \times 10^{-4} = 0.02. \quad (6)$$

In the above, we have used the average yield of heavy strange and antistrange mesons as well as that of heavy baryons and antibryons to remove the effect of baryon and strangeness chemical potentials. A similar analysis for heavy ion collisions at LHC based on the charm and bottom quark numbers $N_c = 20$ and $N_b = 0.8$ (see Table I) gives the charm and bottom fugacities $\gamma_c = 15.8$ and $\gamma_b = 3.3 \times 10^7$, respectively. These values together with those for RHIC are given in Table II.

In Table II, we also show the yield N_K ($N_{\bar{K}}$) of K ($\bar{K}$) mesons given as a sum of the directly produced K ($\bar{K}$) and

TABLE II. Fugacities for c and b quarks and hadron numbers from the statistical model at thermal freeze-out temperature T_F and volume V_F in central heavy ion collisions at RHIC and LHC, including contributions from resonance decays shown in the fourth column.

	RHIC	LHC	
γ_c	6.40	15.8	
γ_b	2.2×10^6	3.3×10^7	
N_K	142	363	K, K^*
$N_{\bar{K}}$	127	363	$\bar{K}, \bar{K}^*$
$N_D = N_{\bar{D}}$	1.0	6.9	
$N_{D^*} = N_{\bar{D}^*}$	1.5	10	
N_{D_1}	0.19	1.3	
$N_B = N_{\bar{B}}$	5.3×10^{-3}	0.21	
$N_{B^*} = N_{\bar{B}^*}$	1.2×10^{-2}	0.49	
N_N	62	150	N, Δ
N_Ξ	4.7	13	
N_Ω	0.81	2.3	
N_{Ξ_c}	0.10	0.65	

those from the strong decay of K^* ($\bar{K}^*$) after their freeze-out. Similarly, the yield of nucleons N_N includes both directly produced N and those from the strong decay of Δ. These results are obtained by using the Fermi-Dirac and Bose-Einstein distributions in Eq. (1). We note that approximating these distributions by the Boltzmann distribution as given in Eq. (2) does not introduce a large error (at most 1% for exotic hadrons), while the nonrelativistic approximation used in Eq. (3) leads to an error of about 30–40%.

C. The coalescence model

The coalescence model for particle production in nuclear reactions is based on the sudden approximation by calculating the overlap of the density matrix of the constituents in an emission source with the Wigner function of the produced particle [34]. The model has been extensively used to study light nuclei production in nuclear reactions [35] as well as hadron production from the QGP produced in relativistic heavy ion collisions [23–25,36]. In the coalescence model, the number of hadrons of certain type h produced from the coalescence of n constituents is given by [24]

$$N_h^{\text{coal}} = g_h \int \left[\prod_{i=1}^{n} \frac{1}{g_i} \frac{p_i \cdot d\sigma_i}{(2\pi)^3} \frac{d^3 \mathbf{p}_i}{E_i} f(x_i, p_i) \right]$$
$$\times f^W(x_1, \ldots, x_n : p_1, \ldots, p_n). \quad (7)$$

In the above equation, g_h is again the degeneracy of the hadron, whereas g_i is that of its ith constituent and $d\sigma_i$ denotes an element of a spacelike hypersurface. The function $f(x_i, p_i)$ is the covariant phase-space distribution function of the constituents in the emission source, and it is normalized to their number, that is,

$$\int p_i \cdot d\sigma_i \frac{d^3 \mathbf{p}_i}{(2\pi)^3 E_i} f(x_i, p_i) = N_i, \quad (8)$$

and the function $f^W(x_1, \ldots, x_n : p_1, \ldots, p_n)$ is the Wigner function of the produced hadron and is defined by

$$f^W(x_1, \ldots, x_n : p_1, \ldots, p_n)$$
$$= \int \prod_{i=1}^{n} dy_i e^{ip_i y_i} \psi^*(x_1 + y_1/2, \ldots, x_n + y_n/2)$$
$$\times \psi(x_1 - y_1/2, \ldots, x_n - y_n/2), \quad (9)$$

in terms of its wave function $\psi(x_1, \ldots, x_n)$.

Following the derivation given in Refs. [18,19], where the nonrelativistic limit is taken and the hadron wave functions are assumed to be those of a spherically symmetric harmonic oscillator, the above equation can be reduced to

$$N_h^{\text{coal}} = g_h \prod_{j=1}^{n} \frac{N_j}{g_j} \prod_{i=1}^{n-1} \frac{\int d^3 y_i d^3 k_i f_i(k_i) f^W(y_i, k_i)}{\int d^3 y_i d^3 k_i f_i(k_i)}, \quad (10)$$

where $f^W(y_i, k_i)$, with y_i and k_i being, respectively, the internal (relative) spatial and momentum coordinates, is the Wigner function associated with the internal (relative) wave function. As in Ref. [19], we assume that the particles in the emission source are uniformly distributed in space and have

momentum distributions $f_j(p_j)$ given by the Boltzmann distribution of temperature T only for the transverse momentum $p_{j,T}$, while the strong Bjorken correlation of equal spatial (η_j) and momentum (Y_j) rapidities is imposed for the longitudinal momentum, that is,

$$f_j(p_j) \propto \delta(Y_j - \eta_j) \exp\left(-\frac{p_{j,T}^2}{2m_j T} \right), \quad (11)$$

with $\eta_j = \ln[(t_j + z_j)/(t_j - z_j)]/2$ and $Y_j = \ln[(E_j + p_{j,z})/(E_j - p_{j,z})]/2$ being the space-time and momentum-energy rapidities, respectively. From the relation

$$\prod_{j=1}^{n} \exp\left(-\frac{p_{j,T}^2}{2m_j T} \right) = \exp\left(-\frac{P_T^2}{2MT} \right) \prod_{i=1}^{n-1} \tilde{f}_i(k_i), \quad (12)$$

with P_T and M denoting the total transverse momentum and the total mass, respectively, we then obtain the two-dimensional momentum distribution function of the constituents in Jacobi coordinates, $\tilde{f}_i(k_i)$,

$$\tilde{f}_i(k_i) \propto \exp\left(-\frac{k_i^2}{2\mu_i T} \right), \quad (13)$$

where the reduced constituent masses μ_i are defined by

$$\frac{1}{\mu_i} = \frac{1}{m_{i+1}} + \frac{1}{\sum_{j=1}^{i} m_j}, \quad (14)$$

or, explicitly,

$$\mu_1 = \frac{m_1 m_2}{m_1 + m_2}, \quad \mu_2 = \frac{m_3(m_1 + m_2)}{m_1 + m_2 + m_3},$$
$$\mu_3 = \frac{m_4(m_1 + m_2 + m_3)}{m_1 + m_2 + m_3 + m_4}, \quad (15)$$
$$\mu_4 = \frac{m_5(m_1 + m_2 + m_3 + m_4)}{m_1 + m_2 + m_3 + m_4 + m_5}, \text{ etc.}$$

In the nonrelativistic limit, the rapidity variables are simplified at midrapidities ($Y = \eta \sim 0$) as $\eta_j \simeq z_j/t_j$ and $Y_j \simeq p_{j,z}/m_j$. We can thus omit the contribution from the longitudinal momentum in the Wigner function f^W as long as the time where the coalescence takes place after the collision is large compared with the internal time scale of the hadron, $t_j \gg 1/\omega$, where ω is the oscillator frequency. In this case, the three-dimensional momentum integrations in Eq. (10) reduces to two-dimensional ones over $\tilde{f}_i(k_i)$ and the Wigner functions in transverse momentum k_i. The latter are given explicitly as

$$f_s^W(y_i, k_i) = 8 \exp\left(-\frac{y_i^2}{\sigma_i^2} - k_i^2 \sigma_i^2 \right),$$

$$f_p^W(y_i, k_i) = \left(\frac{16}{3} \frac{y_i^2}{\sigma_i^2} - 8 + \frac{16}{3} \sigma_i^2 k_i^2 \right) \exp\left(-\frac{y_i^2}{\sigma_i^2} - k_i^2 \sigma_i^2 \right)$$

$$f_d^W(y_i, k_i) = \frac{16}{30} \left[4 \frac{y_i^4}{\sigma_i^4} - 20 \frac{y_i^2}{\sigma_i^2} + 15 - 20\sigma_i^2 k_i^2 + 4\sigma_i^4 k_i^4 \right.$$
$$\left. + 16 y_i^2 k_i^2 - 8(\vec{y}_i \cdot \vec{k}_i)^2 \right] \exp\left(-\frac{y_i^2}{\sigma_i^2} - k_i^2 \sigma_i^2 \right),$$
$$(16)$$

for the s wave, p wave, and d wave, respectively, with the parameters $\sigma_i = 1/\sqrt{\mu_i \omega}$ related to the oscillator frequency ω and the reduced constituent masses μ_i. In Appendix A, we derive the Wigner function for the d-wave state from the harmonic oscillator wave functions.

Carrying out the phase-space integrals in Eq. (10) as shown in Appendix B, we obtain the coalescence factor for each relative coordinate,

$$
\begin{aligned}
F(\sigma_i, \mu_i, l_i, T) &\equiv \frac{\int d^3 y_i d^2 k_i \, \tilde{f}_i(k_i) f^W(y_i, k_i)}{\int d^2 k_i \, \tilde{f}_i(k_i)} \\
&= \frac{(4\pi\sigma_i^2)^{3/2}}{1 + 2\mu_i T \sigma_i^2} \frac{(2l_i)!!}{(2l_i + 1)!!} \left[\frac{2\mu_i T \sigma_i^2}{1 + 2\mu_i T \sigma_i^2} \right]^{l_i},
\end{aligned}
\tag{17}
$$

where l_i is the angular momentum of the wave function associated with the relative coordinate y_i. Combining these results, we obtain the following simple expression for the yield of hadrons from the coalescence model:

$$
\begin{aligned}
N_h^{\text{coal}} &\simeq g V \prod_{j=1}^{n} \frac{N_j}{g_j V} \prod_{i=1}^{n-1} F(\sigma_i, \mu_i, l_i, T) \\
&\simeq g V \prod_{j=1}^{n} \frac{N_j}{g_j V} \prod_{i=1}^{n-1} \frac{(4\pi\sigma_i^2)^{3/2}}{1 + 2\mu_i T \sigma_i^2} \\
&\quad \times \frac{(2l_i)!!}{(2l_i + 1)!!} \left[\frac{(2\mu_i T \sigma_i^2)}{(1 + 2\mu_i T \sigma_i^2)} \right]^{l_i} \\
&\simeq \frac{g V (M\omega)^{3/2}}{(4\pi)^{3/2}} \frac{(2T/\omega)^L}{(1 + 2T/\omega)^{n+L-1}} \\
&\quad \times \prod_{j=1}^{n} \frac{N_j (4\pi)^{3/2}}{g_j V (m_j \omega)^{3/2}} \prod_{i=1}^{n-1} \frac{(2l_i)!!}{(2l_i + 1)!!},
\end{aligned}
\tag{18}
$$

where l_i is 0 for an s-wave, 1 for a p-wave, and 2 for a d-wave constituent, $L = \sum_{i=1}^{n-1} l_i$, and $M = \sum_{i=1}^{n} m_i$. Here we have used the relation $\mu_i \sigma_i^2 = 1/\omega$ to convert the main dependence on l_i into the form of the orbital angular momentum sum L. For $L \geqslant 2$, the last factor in Eq. (18) depends on the way L is decomposed into l_i. For example, for $L = 2$ and $n = 3$, the combination $(l_1, l_2) = (1, 1)$ gives a factor 4/9, while $(l_1, l_2) = (2, 0)$ leads to a factor 8/15.

1. Quark coalescence

To apply the coalescence model to hadron production from the QGP at the critical temperature T_c when the volume is V_C, we need to fix the oscillator frequency appropriately. This is done by choosing the oscillator frequencies for light, strange, charmed, and bottom hadrons (ω, ω_s, ω_c, and ω_b) in the quark coalescence to reproduce the yields of reference normal hadrons in the statistical model. These values are then used to predict the yields of exotic hadrons.

For hadrons composed of light (up and down) quarks, we take the oscillator frequency $\omega = 550$ MeV to obtain in the coalescence model similar ω and ρ yields as in the statistical model as shown in Table III.

For hadrons composed of light and strange quarks, the parameter ω_s in the coalescence model is determined by fitting the statistical model prediction for $\Lambda(1115)$ including the contribution from resonance decays. Taking into account states in the octet and decuplet representations that decay dominantly to $\Lambda(1115)$, we obtain the following result for heavy ion collisions at RHIC:

$$
\begin{aligned}
N_{\Lambda(1115)}^{\text{stat,total}} &= N_{\Lambda(1115)}^{\text{stat}} + \frac{1}{3} N_{\Sigma(1192)}^{\text{stat}} + N_{\Xi(1318)}^{\text{stat}} \\
&\quad + \left(0.87 + \frac{0.11}{3}\right) N_{\Sigma(1385)}^{\text{stat}} + N_{\Xi(1530)}^{\text{stat}} + N_{\Omega^-(1672)}^{\text{stat}} \\
&= 6.46 + \frac{1}{3} \times 13.57 + 4.73 + \left(0.87 + \frac{0.11}{3}\right) \\
&\quad \times 10.91 + 3.42 + 0.81 \\
&= 29.8.
\end{aligned}
\tag{19}
$$

In the above formula, 0.87 and 0.11/3 in the parentheses represent, respectively, the branching ratios of $\Sigma(1385) \to \Lambda + \pi$ and $\Sigma(1385) \to \Sigma^0 + \pi$ in the $\Sigma(1385)$ decay. All numbers are calculated at T_H and V_H with $\mu_s = 10$ MeV and $\mu_B = 20$ MeV for RHIC. To reproduce the total yield within the coalescence model with the constituent quark masses $m_{u,d} = 300$ MeV and $m_s = 500$ MeV, we need $\omega_s = 519$ MeV after taking into account the same feed-down contributions as in Eq. (19). Specifically, we have from the coalescence model

$$
\begin{aligned}
N_{\Lambda(1115)}^{\text{coal,total}} &= 3.01 + \frac{1}{3} \times 9.03 + 2.20 + \left(0.87 + \frac{0.11}{3}\right) \\
&\quad \times 18.07 + 4.40 + 0.78 \\
&= 29.8.
\end{aligned}
\tag{20}
$$

We use this parameter to estimate the yield of other hadrons that are composed of light quarks and strange quarks. As shown in Table III, this value leads to a yield of $\Lambda(1520)$, which has the s quark in the p-wave state, in the coalescence model that is smaller than that in the statistical model as first pointed out in Ref. [32].

The oscillator frequency for charmed hadrons is fixed to reproduce the $\Lambda_c(2286)$ yield including the feed-down contribution [37] but without taking into consideration the effect of the diquarks [38]. For the $\Lambda_c(2286)$ yield, we consider only the contribution from $\Sigma_c(2455)$, $\Sigma_c(2520)$, and $\Lambda_c(2625)$ decays as states of higher masses are negligible; that is,

$$
\begin{aligned}
N_{\Lambda_c(2286)}^{\text{stat,total}} &= N_{\Lambda_c(2286)}^{\text{stat}} + N_{\Sigma_c(2455)}^{\text{stat}} + N_{\Sigma_c(2520)}^{\text{stat}} \\
&\quad + 0.67 \times N_{\Lambda_c(2625)}^{\text{stat}} \\
&= 0.139 + 0.177 + 0.254 + 0.67 \times 0.048 \\
&= 0.602,
\end{aligned}
\tag{21}
$$

at RHIC. Fitting again the total yield of $\Lambda_c(2286)$ calculated in the statistical model to that in the coalescence model for the same resonances as given in Eq. (21),

$$
\begin{aligned}
N_{\Lambda_c(2286)}^{\text{coal,total}} &= 0.058 + 0.173 + 0.346 + 0.67 \times 0.037 \\
&= 0.602,
\end{aligned}
\tag{22}
$$

we obtain $\omega_c = 385$ MeV for the charm quark mass $m_c = 1500$ MeV.

TABLE III. Yields of normal hadrons at RHIC and LHC in the coalescence and statistical models with oscillator frequencies $\omega = 550$ MeV, $\omega_s = 519$ MeV, $\omega_c = 385$ MeV, and $\omega_b = 338$ MeV are determined by fitting the statistical model results for $\Lambda(1115)$, $\Lambda_c(2286)$, and $\Lambda_b(5620)$ marked with * at RHIC after taking account of resonance decays. Numbers in the parentheses are those without the decay contribution.

Configuration	Particle	RHIC		LHC	
		Coalescence	Statistical	Coalescence	Statistical
$\bar{q}q$	$\omega(782)$	44.2	40.2	119	108
	$\rho(770)$	132	127	358	342
	$\bar{K}^*(892)$	41.2	47.2	111	135
	$K^*(892)$	41.2	52.9	111	135
qqs	$\Lambda(1115)$	29.8*	29.8	80.5	77.5
		(3.0)	(6.5)	(8.1)	(16.5)
	$\Lambda(1520)$	1.6	1.9	4.4	4.8
qqQ	$\Lambda_c(2286)$	0.60*	0.60	4.0	3.6
		(0.058)	(0.14)	(0.39)	(0.83)
	$\Lambda_b(5620)$	3.6×10^{-3}*	3.6×10^{-3}	0.14	0.13
		(3.6×10^{-4})	(9.2×10^{-4})	(0.014)	(0.033)

The oscillator frequency for bottom hadrons $\omega_b = 338$ MeV is obtained by fitting the sum of the statistical model results for $\Lambda_b(5620)$ and the contribution from $\Sigma_b(5810)$ and $\Sigma_b^*(5830)$ decays at RHIC,

$$N_{\Lambda_b(5620)}^{\text{stat,total}} = N_{\Lambda_b(5620)}^{\text{stat}} + N_{\Sigma_b(5810)}^{\text{stat}} + N_{\Sigma_b(5830)}^{\text{stat}}$$
$$= 9.2 \times 10^{-4} + 9.7 \times 10^{-4} + 1.73 \times 10^{-3}$$
$$= 3.62 \times 10^{-3}, \tag{23}$$
$$N_{\Lambda_b(5620)}^{\text{coal,total}} = 3.62 \times 10^{-4} + 1.085 \times 10^{-3} + 2.170 \times 10^{-3}$$
$$= 3.62 \times 10^{-3}, \tag{24}$$

with the bottom quark mass $m_b = 4700$ MeV.

Because the oscillator frequencies are related to the sizes of hadrons [18,19], the same values as determined at RHIC are used in the coalescence calculations for heavy ion collisions at LHC. Using the same ω values as those for normal hadrons, we then see from Eq. (18) that the addition of a s-wave, p-wave, or d-wave quark leads to, respectively, a coalescence factor

$$\frac{1}{g_i} \frac{N_i}{V} \frac{\left(4\pi\sigma_i^2\right)^{3/2}}{\left(1 + 2\mu_i T \sigma_i^2\right)} \sim 0.360,$$

$$\frac{1}{g_i} \frac{N_i}{V} \frac{2}{3} \frac{\left(4\pi\sigma_i^2\right)^{3/2} 2\mu_i T \sigma_i^2}{\left(1 + 2\mu_i T \sigma_i^2\right)^2} \sim 0.093,$$

$$\frac{1}{g_i} \frac{N_i}{V} \frac{8}{15} \frac{\left(4\pi\sigma_i^2\right)^{3/2} \left(2\mu_i T \sigma_i^2\right)^2}{\left(1 + 2\mu_i T \sigma_i^2\right)^3} \sim 0.029. \tag{25}$$

The production of multiquark hadrons involves more s-, p-, and d-wave coalescence factors and is hence generally suppressed. Moreover, the d-wave coalescence is suppressed in comparison with the p-wave coalescence, which is further suppressed relative to the s-wave coalescence [32].

2. Hadron coalescence

For the yields of weakly bound hadronic molecules from the coalescence of hadrons, they are evaluated at the kinetic freeze-out temperature T_F and volume V_F. The oscillator frequencies needed for hadronic molecules in the hadron coalescence is related to their mean square distances $\langle r^2 \rangle$ between the two constituent hadrons. For a hadronic molecule in the relative s-wave state, the oscillator frequency is given by

$$\omega = \frac{3}{2\mu_R \langle r^2 \rangle}, \tag{26}$$

where $\mu_R = m_1 m_2/(m_1 + m_2)$ is the reduced mass. The mean square distance of the hadronic molecule can be further related to its binding energy B via the scattering length a_0 of the two interacting constituent hadrons, that is,

$$B \simeq \frac{\hbar^2}{2\mu_R a_0^2}, \quad \langle r^2 \rangle \simeq \frac{a_0^2}{2}, \tag{27}$$

These relations are valid when the binding energy is small and the scattering length is large compared to the range of the hadronic interaction, and they can be easily obtained as follows. Using the relation $k \cot \delta_0(k) = -1/a_0$ for the relative momentum $k \to 0$ between the s-wave scattering phase shift δ_0 and the scattering length a_0, the S matrix for two interacting hadrons at low energies can be approximated as

$$S = e^{2i\delta_0(k)} \approx \frac{-\frac{1}{a_0} + ik}{-\frac{1}{a_0} - ik}, \tag{28}$$

which has a pole at $k = i/a_0$, corresponding to a bound state with the binding energy given by the first equation in Eq. (27) and the radial wave function outside the interaction range $u_b(r) \sim e^{-r/a_0}$. Assuming that a_0 is much larger than the interaction range and using the above form of the wave function for the whole region, we obtain the mean square distance given by the second equation in Eq. (27). For a weakly bound two-body state, we thus obtain from Eqs. (26) and (27) the simple relation $\omega = 6B$. We note that $\langle r^2 \rangle$ is the mean

square distance in the relative coordinate, and it is not the squared mean radius from the center of mass.

For example, the oscillator frequency for $f_0(980)$ can be obtained from $\omega_{f_0(980)} = 6 \times B_{f_0(980)} = 67.8$ MeV with $B_{f_0(980)} = M_{K^+} + M_{\bar{K}_0} - M_{f_0(980)} = 493.7 + 497.6 - 980 = 11.3$ MeV. As another example, the oscillator frequency $\omega_{\Omega\Omega}$ for the diomega $(\Omega\Omega)_{0^+}$ predicted by the chiral quark model [39] can be calculated from Eq. (26),

$$\omega_{\Omega\Omega} = \frac{3}{2\mu_{\Omega\Omega}\langle r^2\rangle_{\Omega\Omega}} = \frac{3}{2}\frac{197.3^2}{1672.45/2 \times 0.84^2}$$
$$= 98.8 \text{MeV}, \quad (29)$$

where $\sqrt{\langle r^2\rangle}_{\Omega\Omega} = 0.84$ fm [39] has been used. By the same token, we can calculate the oscillator frequencies for all the hadronic molecules, and the results are summarized in Table IV.

III. EXOTIC HADRONS

In this section, we briefly discuss the properties, such as the quantum numbers and possible decay modes, and the current theoretical and experimental status of the exotic hadrons included in the present study. For convenience, we classify these hadrons into exotic mesons (Sec. III A), exotic baryons (Sec. III B) and exotic dibaryons (Sec. III C), as shown in Table IV.

A. Exotic mesons

For exotic mesons, we include the following.

(1) $f_0(980)$: This $I = 0$ scalar particle together with the $I = 1$ $a_0(980)$ are members of the scalar nonet that has been thought to be composed of multiquark configurations [7,8]. If $f_0(980)$ is a member of the multiquark configurations, its wave function then has a hidden $\bar{s}s$ component. Assuming that they are composed of a quark-antiquark pair, their wave functions would be $f_0(980) \sim s\bar{s}$ and $a_0(980) \sim (u\bar{u} - d\bar{d})/\sqrt{2}$. An early QCD sum rule analysis suggested, however, that $f_0(980)$ and $a_0(980)$ were just the $I = 0$ and 1 combinations of $u\bar{u}$ and $d\bar{d}$ [40]. There are also models in which $f_0(980)$ is a $K\bar{K}$ molecule [41] and is a dynamically generated state in the $\pi\pi$ and $\bar{K}K$ channels [42]. While there seems to be

TABLE IV. List of exotic hadrons discussed in this paper. Shown are the mass (m), degeneracy (g), isospin (I), spin and parity (J^P), the quark structure ($2q/3q/6q$ and $4q/5q/8q$), molecular configuration (Mol.) and corresponding oscillator frequency ($\omega_{\text{Mol.}}$), and decay mode of a hadron. For the $\omega_{\text{Mol.}}$, it is fixed by the binding energies B of hadrons [$\omega \simeq 6 \times B$, marked (B)] or their mean square distances $\langle r^2\rangle$ [$\omega \simeq 3/2\mu\langle r^2\rangle$, marked (R)]. In the case of three-body molecular configurations for exotic dibaryons, we adopt the $\omega_{\text{Mol.}}$ as that for the subsystem, as marked (T).

Particle	m (MeV)	g	I	J^P	$2q/3q/6q$	$4q/5q/8q$	Mol.	$\omega_{\text{Mol.}}$ (MeV)	Decay mode
Mesons									
$f_0(980)$	980	1	0	0^+	$q\bar{q}, s\bar{s}(L=1)$	$q\bar{q}s\bar{s}$	$\bar{K}K$	67.8(B)	$\pi\pi$ (Strong decay)
$a_0(980)$	980	3	1	0^+	$q\bar{q}(L=1)$	$q\bar{q}s\bar{s}$	$\bar{K}K$	67.8(B)	$\eta\pi$ (Strong decay)
$K(1460)$	1460	2	1/2	0^-	$q\bar{s}$	$q\bar{q}q\bar{s}$	$\bar{K}KK$	69.0(R)	$K\pi\pi$ (Strong decay)
$D_s(2317)$	2317	1	0	0^+	$c\bar{s}(L=1)$	$q\bar{q}c\bar{s}$	DK	273(B)	$D_s\pi$ (Strong decay)
T_{cc}^{1} [a]	3797	3	0	1^+	—	$qq\bar{c}\bar{c}$	$\bar{D}\bar{D}^*$	476(B)	$K^+\pi^- + K^+\pi^- + \pi^-$
$X(3872)$	3872	3	0	$1^+, 2^-$ [c]	$c\bar{c}(L=2)$	$q\bar{q}c\bar{c}$	$\bar{D}D^*$	3.6(B)	$J/\psi\pi\pi$ (Strong decay)
$Z^+(4430)$ [b]	4430	3	1	0^- [c]	—	$q\bar{q}c\bar{c}(L=1)$	$D_1\bar{D}^*$	13.5(B)	$J/\psi\pi$ (Strong decay)
T_{cb}^{0} [a]	7123	1	0	0^+	—	$qq\bar{c}\bar{b}$	$\bar{D}B$	128(B)	$K^+\pi^- + K^+\pi^-$
Baryons									
$\Lambda(1405)$	1405	2	0	$1/2^-$	$qqs(L=1)$	$qqs\bar{q}$	$\bar{K}N$	20.5(R)–174(B)	$\pi\Sigma$ (Strong decay)
$\Theta^+(1530)$ [b]	1530	2	0	$1/2^+$ [c]	—	$qqqq\bar{s}(L=1)$	—	—	KN (Strong decay)
$\bar{K}KN$ [a]	1920	4	1/2	$1/2^+$	—	$qqqs\bar{s}(L=1)$	$\bar{K}KN$	42(R)	$K\pi\Sigma, \pi\eta N$ (Strong decay)
$\bar{D}N$ [a]	2790	2	0	$1/2^-$	—	$qqqq\bar{c}$	$\bar{D}N$	6.48(R)	$K^+\pi^-\pi^- + p$
$\bar{D}^*N$ [a]	2919	4	0	$3/2^-$	—	$qqqq\bar{c}(L=2)$	$\bar{D}^*N$	6.48(R)	$\bar{D} + N$ (Strong decay)
Θ_{cs} [a]	2980	4	1/2	$1/2^+$	—	$qqqs\bar{c}(L=1)$	—	—	$\Lambda + K^+\pi^-$
BN [a]	6200	2	0	$1/2^-$	—	$qqqq\bar{b}$	BN	25.4(R)	$K^+\pi^-\pi^- + \pi^+ + p$
B^*N [a]	6226	4	0	$3/2^-$	—	$qqqq\bar{b}(L=2)$	B^*N	25.4(R)	$B + N$ (Strong decay)
Dibaryons									
H [a]	2245	1	0	0^+	$qqqqss$	—	ΞN	73.2(B)	$\Lambda\Lambda$ (Strong decay)
$\bar{K}NN$ [b]	2352	2	1/2	0^- [c]	$qqqqqs(L=1)$	$qqqqqq\,s\bar{q}$	$\bar{K}NN$	20.5(T)–174(T)	ΛN (Strong decay)
$\Omega\Omega$ [a]	3228	1	0	0^+	$ssssss$	—	$\Omega\Omega$	98.8(R)	$\Lambda K^- + \Lambda K^-$
H_c^{++} [a]	3377	3	1	0^+	$qqqqsc$	—	$\Xi_c N$	187(B)	$\Lambda K^-\pi^+\pi^+ + p$
$\bar{D}NN$ [a]	3734	2	1/2	0^-	—	$qqqqqq\,q\bar{c}$	$\bar{D}NN$	6.48(T)	$K^+\pi^- + d, K^+\pi^-\pi^- + p + p$
BNN [a]	7147	2	1/2	0^-	—	$qqqqqq\,q\bar{b}$	BNN	25.4(T)	$K^+\pi^- + d, K^+\pi^- + p + p$

[a]Particles that are newly predicted by theoretical models.
[b]Particles that are not yet established.
[c]Undetermined quantum numbers of existing particles.

consensus from lattice calculations that this particle is a tetraquark state, the situation is not at all clear because of the treatment of disconnected diagrams [43].

(2) $K(1460)$: This is an exited state of kaon with $J^P = 0^-$ on the particle list of the Particle Data Group (PDG) but is omitted from the summary table [44]. It was observed in the partial-wave analysis of the $K\pi\pi$ final state in elementary reactions. Recently, this resonance has been studied theoretically in the context of the meson dynamics. In Ref. [45] this kaon was obtained from the K-$f_0(980)$ s-wave two-body dynamics with the $f_0(980)$ dynamically generated in the $\bar{K}K$ and $\pi\pi$ coupled channels. A later study in Ref. [46] considered the three-body coupled-channel dynamics of $\bar{K}KK$ in a Faddeev approach and found a very similar kaonic excitation. A nonrelativistic potential model for the $\bar{K}KK$ system was also used in Ref. [46], and a quasibound state of binding energy 21 MeV and root-mean-square radius 1.6 fm was obtained. Thus, the $K(1460)$ could be understood as a $\bar{K}KK$ hadronic molecular state.

(3) $D_{sJ}(2317)$: This state predicted in Refs. [47,48] was first observed by the BaBar Collaboration [2] through the $D_s^+\pi^0$ channel in inclusive e^+e^- annihilation. Its measured mass is approximately 160 MeV below the prediction of the very successful quark model for the charmed meson [49]. Owing to its low mass, the structure of $D_{sJ}(2317)$ has been under extensive debate. It has been interpreted as a $c\bar{s}$ state [50–54], two-meson molecular state [55–61], $D-K$ mixing [62], four-quark state [63–66], or a mixture of two-meson and four-quark states [67].

(4) $T_{cc}^1(ud\bar{c}\bar{c})$: The set of tetraquarks with two heavy quarks were first considered in Ref. [68]. The structure with [ud] diquark is expected to be particularly stable [69,70] and could be bound against the strong decay into D_1D. The quantum number is $J^P = 1^+$ with $I = 0$; hence, the decay into DD is forbidden owing to the angular momentum conservation. Estimates based on the simple color-spin interaction suggest the mass to be 3796 MeV [14,15]. The hadronic decay mode of T_{cc} is $D^{*-}\bar{D}^0$ if its mass is above the threshold and $\bar{D}^0D^0\pi^-$ if below. If the T_{cc} is strongly bound, it can then decay weakly to $D^{*-}K^+\pi^-$ with a lifetime similar to that of the $\bar{D}$ meson. A molecular state with the same quantum number was also predicted to exist within the pion-exchange model [71]. The production of doubly charmed hadrons in heavy ion collisions at RHIC was discussed in Ref. [72], and also estimated for LHC [14]. This state could also be searched for at Belle. In particular, the search should be similar to that for the doubly charmed baryon such as the Ξ_{cc}. Here are the two possibilities. The first one is through the decay of the B meson. Unfortunately, the search at Belle was not successful [73] as the dominant subprocess was the weak decay of the $\bar{b}$ quark into a $\bar{c}$ by emitting a $W^+(\to c\bar{s})$. Therefore, while the $c\bar{c}$ is produced, the cc creation might be highly suppressed. However, another more feasible search is in the continuum background where two $c\bar{c}$ pairs are known to be produced in the reaction $e^+e^- \to J/\psi X(3940)$ [74].

(5) $X(3872)$: The Belle collaboration found this particle in the $B^+ \to X(3872)K^+ \to J/\psi\pi^+\pi^-K^+$ decay [3]. CDF, D0, and BaBar have confirmed its existence, and the current world average mass is 3871.2 ± 0.39 MeV. Although the new BaBar result favors the $J^{PC} = 2^{-+}$ assignment [75], the established properties of the $X(3872)$ are in conflict with this assignment [76,77]. Therefore, the favored quantum numbers are $J^{PC} = 1^{++}$ with the isospin violating decay modes. This particle was predicted in Ref. [78] as a $D\bar{D}^{*0}$ bound state within a meson-exchange model. It was shown in this study that in the $D\bar{D}^*$ sector the one-pion exchange interaction alone is strong enough to form a molecular state that is bound by approximately 50 MeV. In this case, other molecular states of $D^*\bar{D}^*$, $D_1\bar{D}^*$, $D_1\bar{D}$, and $D_0\bar{D}$ are also expected to exist as the pion exchange is allowed in these channels as well. In other studies, it has been claimed that the $X(3872)$ has the admixture of the $\bar{c}c$ component and is thus a tetraquark hadron [5]. We note that, because the quantum number of isosinglet and $J^{PC} = 1^{++}$ (or 2^{-+}) for the $X(3872)$ is the same as that of the quarkonium state, it is a cryptoexotic state (for another example, see Ref. [79]). Its dominant decay modes include $J/\psi\pi^+\pi^-$, $J/\psi\pi^+\pi^-$, and $D^0\bar{D}\pi^0$.

(6) $Z^+(4430)$: The Belle collaboration observed this charged state in $B^+ \to K\psi'\pi^+$ through its decay into $\psi'\pi^+$ [4]. The reported mass and width are $M = 4433$ MeV and $\Gamma = 45^{+18+30}_{-13-13}$ MeV, respectively. The reported mass is close to the $D_1\bar{D}^*$ threshold and hence the possible structure for this state is either a molecular or a tetraquark state [5]. As commented in the discussion on $X(3872)$, the one-pion exchange interaction could bound a $D_1\bar{D}^*$ molecular state. So far, no other experiment has confirmed this finding. In particular, BaBar [80] also searched the $Z^-(4430)$ signature in four decay modes: $B \to \psi\pi^-K$, where $\psi = J/\psi$ or ψ' and $K = K_S^0$ or K^+. No significant evidence for a signal peak was found in any of the investigated processes. After the failure of the BaBar collaboration in confirming the $Z^-(4430)$ mass peak, Belle performed a reanalysis of their data that took detailed account of possible reflections from the $K\pi^-$ channel. From a full Dalitz plot reanalysis of their data, Belle has confirmed the observation of the $Z^+(4430)$ signal with a 6.4σ peak significance. The updated $Z^+(4430)$ parameters are $M = (4433^{+15+19}_{-12-13})$MeV and $\Gamma = (109^{+86+74}_{-43-56})$MeV [81]. If confirmed, the $Z^+(4430)$ is the first prime candidate for an exotic particle. Considering the $Z^+(4430)$ as a loosely bound s-wave $D_1\bar{D}^*$ molecular state, the allowed angular momentum and parity are $J^P = 0^-, 1^-, 2^-$, although the 2^- assignment is probably suppressed in the $B^+ \to Z^+K$ decay by the small phase space. Among the remaining possible 0^- and 1^- states, the former will be more stable as the latter can also decay to $D_1\bar{D}$ in s wave. Hence the 0^- quantum number is favored.

Very recently the BELLE collaboration [82] reported the observation of two narrow charged structures in the hidden-bottom decay channels $\pi^\pm\Upsilon(nS)(n = 1, 2, 3)$ and $\pi^\pm h_b(mP)(m = 1, 2)$ of $\Upsilon(5S)$. The measured masses (widths) of these two structures are, in units of MeV,

$M_{Z_b} = 10\,610$ ($\Gamma_{Z_b} = 15.6 \pm 2.5$) and $M_{Z_b'} = 10\,650$ ($\Gamma_{Z_b'} = 14.4 \pm 3.2$), respectively. The analysis of the Z_b states decay in the channel $Z_b^{\pm} \rightarrow \Upsilon(2S)\pi^{\pm}$ favors the $I^G(J^P) = 1^+(1^+)$ assignment. Because the masses of these two states are very close to the $\bar{B}B^*(10\,604.6\ \text{MeV})$ and $\bar{B}^*B^*(10\,650.2\ \text{MeV})$ thresholds, they are ideal candidates for these molecular states. It is interesting to notice that the decay channels of the $Z_b^{\pm}$ states are very similar to the decay channel of $Z^+(4430)$.

(7) $T_{cb}^0(ud\bar{c}\bar{b})$: Both the light diquark and heavy anti-diquark are scalar diquarks so that $J^P = 0^+$ with $I = 0$. This particle could be strongly bound with a mass of 7149 MeV [15]. As it has the $\bar{D}^0B^0$ component, it can decay weakly via $T_{cb}^0 \rightarrow K^+\pi^- + K^+\pi^-$.

B. Exotic baryons

For exotic baryons, we consider the following.

(1) $\Lambda(1405)$: This resonant state with $I = 0$, $J^P = 1/2^-$, mass 1406 ± 4 MeV, and width 50 ± 2 MeV [44] has been considered as a quasibound state of the $\bar{K}N$ system [10], even before the establishment of the QCD. The modern theoretical approach based on the chiral dynamics within the unitary framework (the chiral unitary approach) [11,12,83–87] also suggests that this resonant state is dynamically generated in the meson-baryon scattering including the $\bar{K}N$ and $\pi\Sigma$ channels and is dominated by the meson-baryon molecular component [88]. The mean square distance between $\bar{K}$ and N in the $\Lambda(1405)$ is evaluated to be $\langle r^2 \rangle = 2.7$ fm^2 in the chiral unitary approach [89], in which the $\Lambda(1405)$ peak appears around 1420 MeV in the $\bar{K}N$ channel. This value leads to a smaller oscillator frequency for the bound state ($\omega_{\text{Mol.}} = 20.5$ MeV) than that fixed by the binding energy with the $\Lambda(1405)$ mass of 1405 MeV. Its dominant decay mode is $\pi\Sigma$ in the $I = 0$ channel, but there may be the possibility of observing it in the $\gamma\Lambda$ decay mode.

(2) $\Theta^+(uudd\bar{s})$: This flavor exotic baryon with strangeness $S = +1$, $J^P = 1/2^+$, and $I = 0$ was predicted in the chiral soliton model [90]. The intriguing features are its light mass of 1540 MeV and narrow width, which partly motivated the first experimental observation by LEPS [13]. Although the LEPS result was confirmed by several other experiments, it was subsequently followed by negative results with high statistics such as in the high-energy collision experiment by PHENIX [91] and the low-energy photoproduction experiment by CLAS [92]. However, the recent LEPS result maintains a positive signal [93], although the interpretation of the result has been questioned in Refs. [94,95]. The most suitable hadronic decay mode for its identification in an inclusive experiment is $\Theta^+ \rightarrow K^0 p$. The production rate in heavy ion collisions has been estimated in the statistical model [96–98] and in the coalescence model [18]. In the quark model, the spin parity of Θ^+ is $1/2^-$ if all five quarks are in the s-wave orbit but is $1/2^+$ after including the strong diquark correlation [99]. The possibility of a $3/2^-$ state

has also been proposed to explain its narrow width [100]. A recent comprehensive QCD sum rule study favors, however, the $3/2^+$ assignment [101].

(3) $\bar{K}KN$: The quasibound state of $\bar{K}KN$ was predicted to be a hadronic molecular state of N^* with a mass of 1910 MeV, $J^P = 1/2^+$ and $I = 1/2$ in the variational calculation using a hadronic two-body potential [102]. This state was confirmed by a coupled-channels Faddeev calculation [103]. It has been interpreted as a coexistence state of the $\Lambda(1405)K$ and $a_0(980)N$ clusters, and its main decay modes are thus the $K\pi\Sigma$ from the $\Lambda(1405)$ decay and the $\pi\eta N$ from the $a_0(980)$ decay. Because the $\bar{K}KN$ is a hadronic molecular state, it has a large spatial distribution. The root mean square radius is found to be 1.7 fm and the interhadron distances are larger than 2 fm [102].

(4) $\bar{D}N(\bar{D}^*N)$ and $BN(B^*N)$: The quark contents of these hadron molecular states are similar to the $\Theta_{c(b)}$ but with the different quantum numbers of $J^P = 1/2^-$ and $I = 0$. Recently, based on the heavy quark symmetry, a pion induced bound $\bar{D}N$-$\bar{D}^*N$ molecular state was predicted to exist with a binding energy of a few MeV below the threshold of 2806 MeV [16]. This is a shallow bound state compared to the deeply bound Θ_c of about 100 MeV below the threshold. An easily identifiable decay mode is $K^+\pi^-\pi^- p$. The BN molecule would be more stable because the heavy quark symmetry amplifies the strong mixing between BN and B^*N and thus suppresses the kinetic energy. The mass of the BN molecule was predicted to be a few tens of MeV below the threshold of 6218 MeV, and the possible weak decay mode is $K^+\pi^-\pi^- + \pi^+ + p$. In a more recent study [17], the $\bar{D}N$ (BN) was also predicted to have a resonance state between the $\bar{D}N$ (BN) and $\bar{D}^*N$ (B^*N) thresholds, with the mass 2929 (6226) MeV and quantum numbers $J^P = 3/2^-$ and $I = 0$. Similar to the $\bar{D}N$ (BN) bound states, this resonance state is induced by the pion exchange within the heavy quark symmetry. This resonance state can also be regarded as a bound state of $\bar{D}^*$ (B^*) and N with respect to the $\bar{D}^*N$ (B^*N) threshold like that of the Feshbach resonance. Its decay width of 19 (0.12) MeV to the $\bar{D}N$ (BN) via the strong interaction is very narrow as a result of the suppression by the d-wave centrifugal barrier in the final $\bar{D}N$ (BN) state. We have fixed the oscillator frequency ω from the root mean square distance, $\sqrt{\langle r^2 \rangle} = 3.8(1.7)$ fm for the $\bar{D}N$ (BN) molecular state [16], and the same ω is used for its excited state, $\bar{D}^*N$ (B^*N).

(5) $\Theta_c(uudd\bar{c})$ and $\Theta_b(uudd\bar{b})$: The bound Skyrmion approach predicted the bound exotic hadron Θ_c with the mass of 2650 MeV and quantum numbers $J^P = 1/2^+$ and $I = 0$ [104]. There was one experiment reporting a positive signal [105] at a mass around 3.1 GeV, but no confirmation exists so far [106]. An easily identifiable decay mode is $K^+\pi^-\pi^- p$ if the state is strongly bound and $D^{*-}p$ if it is a resonant state. Similarly, the Θ_b mass was predicted to be 5207 MeV with the same quantum numbers $J^P = 1/2^+$ and $I = 0$. The possible weak decay mode is $K^+\pi^-\pi^- + \pi^+ + p$.

(6) $\Theta_{cs}(udus\bar{c})$: In the quark model including the color-spin interaction, the $J^P = 1/2^-$ and $I = 0$ five-quark state can be bound and becomes stable against the strong decay [107,108]. The mass is predicted to be 2920–2930 MeV, depending on the model parameters. This state was searched for in the Fermilab E791 experiment through the $\phi\pi p$ mode [109] and the $K^{*0}K^- p$ mode [110], and the results are so far negative.

C. Exotic dibaryons

The exotic dibaryons included in the present study are as follows.

(1) *H* dibaryon: This particle was first predicted in Ref. [9] as a deeply bound state below the $\Lambda\Lambda$ threshold. Despite extensive searches such as in the BNL-E885 experiments [111], deeply bound *H* dibaryons have not been observed. The discovery of the double-Λ hypernucleus ($^6_{\Lambda\Lambda}$He) in the Nagara event [112] finally excluded the possibility of deeply bound *H* dibaryon, as the two Λ particles can decay strongly into the core nucleus and the *H* dibaryon if the *H* mass is below the $\Lambda\Lambda$ threshold by more than the $\Lambda\Lambda$ separation energy ($B_{\Lambda\Lambda} = 7.25 \pm 0.19^{+0.18}_{-0.11}$ MeV) [112]. As a result, we now have only a narrow window for the *H* particle to be bound, $0 < B_H \lesssim 7$ MeV, where B_H is the binding energy of *H* from the $\Lambda\Lambda$ threshold. The reason why the *H* particle does not strongly bind may be attributable to the instanton-induced determinant (Kobayashi-Maskawa-'t Hooft) [113] interaction, which acts repulsively in the *H* channel and may cancel the strong color-spin attraction, as demonstrated in the quark-cluster model [114]. There is, however, still a possibility that the *H* particle exists as a resonance. In the KEK-E522 experiment, an enhancement in the $\Lambda\Lambda$ invariant mass spectrum is observed at 10–20 MeV above the threshold [115], while the significance as a peak is only around 2σ. This peaklike enhancement cannot be explained by the final-state interaction [116]. Recent lattice calculations have suggested that a bound-state pole exists around the SU(3) limit [117]. With the realistic SU(3) breaking, this bound-state pole would be shifted to a weakly bound state or a resonant state between the $\Lambda\Lambda$ and ΞN thresholds. If we apply the low-energy scattering formula [Eq. (27)], the rms radius of the *H* resonance as a bound state of ΞN [115] may be evaluated to be $0.9-1.3$ fm. Another recent lattice QCD calculation based on larger quark masses has also supported the existence for a bound state of dibaryon [118]. However, whether there exists a bound *H* dibaryon at the physical pion mass limit is still under debate [119, 120].

(2) $\bar{K}NN$: Motivated by the existence of the $\Lambda(1405)$ resonance below the $\bar{K}N$ threshold, the possibility of bound $\bar{K}$-nuclear systems was proposed in Ref. [121] based on a phenomenological $\bar{K}N$ potential. Since then, the simplest $\bar{K}NN$ system has been intensively studied both theoretically and experimentally. While the experiment by the FINUDA Collaboration [122] indicates a peak structure at 2255 MeV in the ΛN invariant mass spectrum, the interpretation of the peak as the $\bar{K}NN$ state is still controversial [123]. Recent rigorous few-body calculations for the $\bar{K}NN$ system indicate that the system bounds in the $J^P = 0^-$ and $I = 1/2$ channel [124–127]. With a suitable treatment of the energy dependence of the $\bar{K}N$ interaction, the mass of the $\bar{K}NN$ system is predicted to be about 2350 MeV [128–130]. In heavy ion collisions, this state can be observed in the ΛN or $\pi \Sigma N$ invariant mass spectrum.

(3) $(\Omega\Omega)_{0^+}$: This is a deeply bound six-quark state predicted by the chiral quark model [39,131]. It has a large binding energy of about 116 MeV and a small root-mean-square distance of 0.84 fm between the two Ωs. Because of its large strangeness content, it is stable against strong hadronic decays and possesses the weak decays $(\Omega\Omega)_{0^+} \to \pi^- + \Xi^0 + \Omega^-$ and $(\Omega\Omega)_{0^+} \to \pi^0 + \Xi^- + \Omega^-$ with a mean lifetime estimated to be about four times longer than the free Ω lifetime of 0.822×10^{-10} s. Apart from these conventional decay modes, the nonmesonic decay $(\Omega\Omega)_{0^+} \to \Xi^- + \Omega^-$ is also possible, and the estimated lifetime of $(\Omega\Omega)_{0^+}$ for this process is twice the free Ω lifetime. Thus, instead of direct observation, the $(\Omega\Omega)_{0^+}$ may also be detected in the $\Xi^-\Omega^-$ invariant mass distribution.

(4) H_c^{++}: This dibaryon with $J^P = 0^0$ and $I = 1$ is predicted in Ref. [15]. It is expected to be strongly bound as it is composed of $[ud]$, $[us]$, and $[uc]$ scalar diquarks, and one of which has to break in order for H_c^{++} to fall apart and to decay to $p + \Xi^+$. The lifetime is expected to be similar to that of Ξ^+, and the dominant hadronic weak decay mode is expected to be $p + \Lambda K^- \pi^+ \pi^+$.

(5) $\bar{D}NN$ and BNN: The attractive $\bar{D}N$ and BN interactions would lead to bound $\bar{D}$ and B mesons in the nuclear medium as their binding energies increase with increasing nuclear density. The $\bar{D}NN$ and BNN molecular states predicted in Ref. [16] are thus nuclei with minimum baryon number. The quantum numbers can be $J^P = 0^-$ or 1^- and $I = 0$ with different types of weak decay mode. The $\bar{D}NN$ states have the decay modes $K^+\pi^-\pi^- + p + p$ for 0^- and $K^+\pi^- + d$ for 1^- with all charged particles in the final state, while the BNN states have the decay modes $K^+\pi^- + \pi^+ + p + p$ for 0^- and $K^+\pi^- + \pi^+ + d$ for 1^-. Therefore, the experimental observation of these decays makes it possible to determine both the spins and the parities of these hadronic molecular states.

IV. YIELDS OF EXOTIC HADRONS IN HEAVY ION COLLISIONS

We show in this section the expected yields of exotic hadrons described in the previous section from central Au + Au collisions at $\sqrt{s_{NN}} = 200$ GeV at RHIC and central Pb + Pb collisions at $\sqrt{s_{NN}} = 5.5$ TeV at LHC. They include results for all possible structure configurations, for example, multiquark hadrons and hadronic molecules, calculated from the coalescence model in addition to those estimated from the statistical model. These results are shown in Table V. We also give some discussions on the obtained results.

TABLE V. Exotic hadron yields in central Au + Au collisions at $\sqrt{s_{NN}} = 200$ GeV at RHIC and in central Pb + Pb collisions at $\sqrt{s_{NN}} = 5.5$ TeV at LHC from the quark coalescence ($2q/3q/6q$ and $4q/5q/8q$) and the hadron coalescence (Mol.), as well as from the statistical model (Stat.)

	RHIC				LHC			
	$2q/3q/6q$	$4q/5q/8q$	Mol.	Stat.	$2q/3q/6q$	$4q/5q/8q$	Mol.	Stat.
Mesons								
$f_0(980)$	3.8, 0.73($s\bar{s}$)	0.10	13	5.6	10, 2.0 ($s\bar{s}$)	0.28	36	15
$a_0(980)$	11	0.31	40	17	31	0.83	1.1×10^2	46
$K(1460)$	—	0.59	3.6	1.3	—	1.6	9.3	3.2
$D_s(2317)$	1.3×10^{-2}	2.1×10^{-3}	1.6×10^{-2}	5.6×10^{-2}	8.7×10^{-2}	1.4×10^{-2}	0.10	0.35
$T_{cc}^{1\,a}$	—	4.0×10^{-5}	2.4×10^{-5}	4.3×10^{-4}	—	6.6×10^{-4}	4.1×10^{-4}	7.1×10^{-3}
$X(3872)$	1.0×10^{-4}	4.0×10^{-5}	7.8×10^{-4}	2.9×10^{-4}	1.7×10^{-3}	6.6×10^{-4}	1.3×10^{-2}	4.7×10^{-3}
$Z^+(4430)^b$	—	1.3×10^{-5}	2.0×10^{-5}	1.4×10^{-5}	—	2.1×10^{-4}	3.4×10^{-4}	2.4×10^{-4}
$T_{cb}^{0\,a}$	—	6.1×10^{-8}	1.8×10^{-7}	6.9×10^{-7}	—	6.1×10^{-6}	1.9×10^{-5}	6.8×10^{-5}
Baryons								
$\Lambda(1405)$	0.81	0.11	1.8–8.3	1.7	2.2	0.29	4.7–21	4.2
$\Theta^{+\,b}$	—	2.9×10^{-2}	—	1.0	—	7.8×10^{-2}	—	2.3
$\bar{K}KN^a$	—	1.9×10^{-2}	1.7	0.28	—	5.2×10^{-2}	4.2	0.67
$\bar{D}N^a$	—	2.9×10^{-3}	4.6×10^{-2}	1.0×10^{-2}	—	2.0×10^{-2}	0.28	6.1×10^{-2}
$\bar{D}^*N^a$	—	7.1×10^{-4}	4.5×10^{-2}	1.0×10^{-2}	—	4.7×10^{-3}	0.27	6.2×10^{-2}
Θ_{cs}^a	—	5.9×10^{-4}	—	7.2×10^{-3}	—	3.9×10^{-3}	—	4.5×10^{-2}
BN^a	—	1.9×10^{-5}	8.0×10^{-5}	3.9×10^{-5}	—	7.7×10^{-4}	2.8×10^{-3}	1.4×10^{-3}
B^*N^a	—	5.3×10^{-6}	1.2×10^{-4}	6.6×10^{-5}	—	2.1×10^{-4}	4.4×10^{-3}	2.4×10^{-3}
Dibaryons								
H^a	3.0×10^{-3}	—	1.6×10^{-2}	1.3×10^{-2}	8.2×10^{-3}	—	3.8×10^{-2}	3.2×10^{-2}
$\bar{K}NN^b$	5.0×10^{-3}	5.1×10^{-4}	0.011–0.24	1.6×10^{-2}	1.3×10^{-2}	1.4×10^{-3}	0.026 − 0.54	3.7×10^{-2}
$\Omega\Omega^a$	3.2×10^{-5}	—	1.5×10^{-5}	6.4×10^{-5}	8.6×10^{-5}	—	4.4×10^{-5}	1.9×10^{-4}
$H_c^{++\,a}$	3.0×10^{-4}	—	3.3×10^{-4}	7.5×10^{-4}	2.0×10^{-3}	—	1.9×10^{-3}	4.2×10^{-3}
$\bar{D}NN^a$	—	2.9×10^{-5}	1.8×10^{-3}	7.9×10^{-5}	—	2.0×10^{-4}	9.8×10^{-3}	4.2×10^{-4}
BNN^a	—	2.3×10^{-7}	1.2×10^{-6}	2.4×10^{-7}	—	9.2×10^{-6}	3.7×10^{-5}	7.6×10^{-6}

[a]Particles that are newly predicted by theoretical model.
[b]Particles that are not yet established.

Comparisons of the yields in the $2q/3q/6q$ column to those in the $4q/5q/8q$ column in Table V show that for most of the hadronic states considered here, the yield from the coalescence model for the compact multiquark state is smaller than that for the usual quark configuration as a result of the suppression owing to the coalescence of additional quarks indicated in Eq. (25). For the same state, the yield from the coalescence model for the molecular configuration is, however, larger than that from the statistical model prediction as seen from comparing the yields in the Mol. column to those in the Stat. column in Table V. This is in contrast to high-energy pp collisions, where molecular configurations with small binding energies are hard to be produced at high p_T [132].

To see more clearly the effect of the structure of a hadron on its production in heavy ion collisions, we show in Fig. 1 the ratio of the coalescence model results to those from the statistical model,

$$R_h^{CS} \equiv N_h^{coal}/N_h^{stat}. \qquad (30)$$

Generally, the ratios for the $2q$ and $3q$ configurations are within the range of $0.2 < R_h < 2$ for normal hadrons, which is shown by the gray zone. This also applies to exotic

hadrons with most of the $2q/3q$ configurations, as shown by the triangles. We observe that the coalescence yield for an exotic multiquark hadron (diamonds) is smaller than those for the usual quark configuration and from the statistical model predictions. This is consistent with the naive expectation that the multiquark coalescence becomes suppressed as the quark number increases. The tetraquark states $f_0(980)$ and $a_0(980)$ are typical examples. In these hadrons, tetraquark configurations necessarily involve strange quarks, and they are thus more suppressed. This suppression also applies to the $5q$ states in exotic baryons [$\Lambda(1405)$, $\Theta^+(1530)$, $\bar{K}KN$, and Θ_{cs}] and the $8q$ state in the $\bar{K}NN$.

The yields of hadronic molecules from the hadron coalescence (circles) depend strongly on the sizes of hadrons. For deeply bound and compact hadronic molecules, their yields are comparable to or smaller than the predictions of the statistical model. However, the loosely bound extended molecules would be formed abundantly. One typical example is $\Lambda(1405)$ that are shown in Table IV for the two cases of $\omega = 20.5$ and 174 MeV. The smaller value, corresponding to a small binding [86,87], gives a larger size for the $\Lambda(1405)$. As a result, antikaons produced in heavy ion collisions have larger probabilities of coalescing with nucleons, resulting in

Coalescence / Statistical model ratio at RHIC   Coalescence / Statistical model ratio at LHC
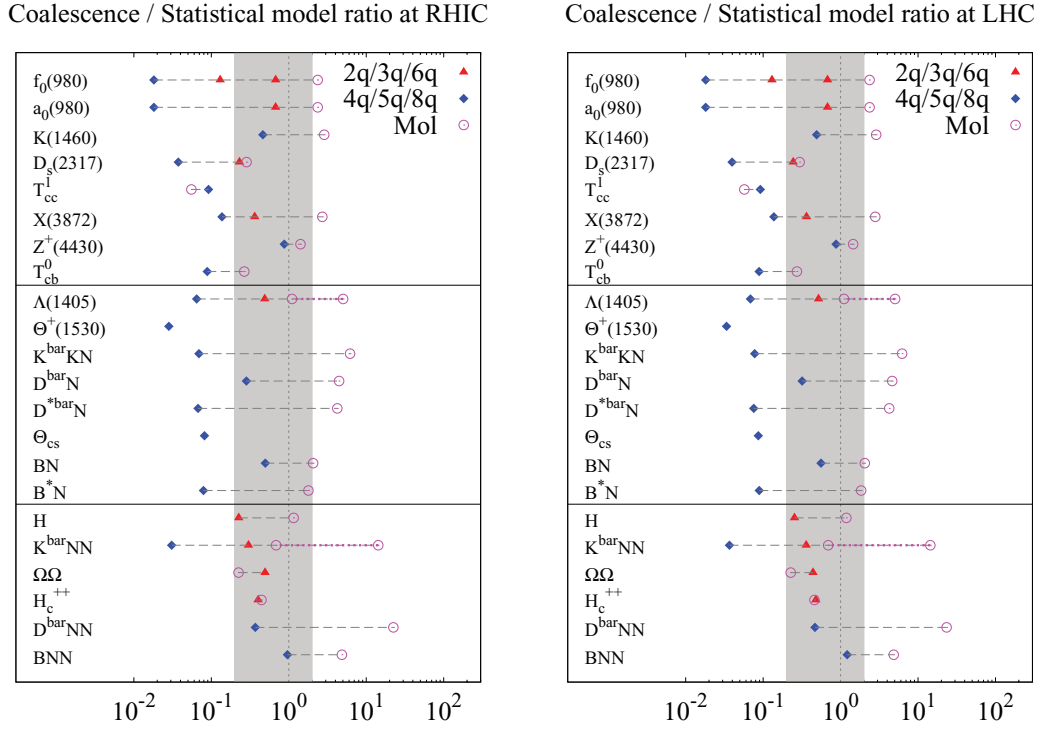

FIG. 1. (Color online) Ratio of the yield of an exotic hadron in the coalescence model to that of the statistical model.

more abundant production of $\Lambda(1405)$. However, for the larger ω value, which corresponds to the case that the pole position of the *S*-matrix for the two-hadron interaction is around 1405 MeV, the $\Lambda(1405)$ can be regarded as a deeply bound state and thus has a smaller size, and hence its yield becomes smaller.

V. DISCUSSIONS

Our results based on the coalescence model for hadron production in relativistic heavy ion collisions have indicated that their yields are strongly dependent on their structures. Therefore, measuring the yields of exotic hadrons allows us to infer the internal configuration of exotic hadrons [20,21]. For example, we have mentioned in Sec. IV A that as possible configurations for $f_0(980)$, quark-antiquark pairs ($\sim s\bar{s}$, $u\bar{u}$, and $d\bar{d}$), a tetraquark state, and a $K\bar{K}$ hadronic molecule have been proposed. To confirm its structure, we refer to preliminary data from the STAR Collaboration for the production yield ratios of $f_0(980)$, π, and ρ^0 [133]. From these results we find that the measured yield of $f_0(980)$ is close to 8, which means that it is more probable for the $f_0(980)$ to be produced as a hadronic molecule state than a tetraquark state (see the order-of-magnitude difference between the yield in the $4q/5q/8q$ column and that in the Mol. column in Table V). Therefore, we conclude that the STAR data seem to rule out a dominant tetraquark configuration for the $f_0(980)$. Further experimental efforts to reduce the error bar are thus highly desirable.

For some exotic hadrons, our results show that the yields are similar for the hadronic and the molecular configuration,

despite the difference in the coalescence temperatures T_C and T_F. This can be attributed to the larger size of the molecular configuration. Assuming other factors are similar, the *s*-wave factors involved in the coalescence at T_F are similar to those at T_C as long as the relevant molecular size is related to the hadron size as $\sigma_C = (V_C/V_F)^{1/3}\sigma_F$ as can be inferred from Eq. (25) after neglecting the temperature dependence in the denominator. If we additionally assume that the volume scales as $V \propto T^{-3}$, we find that the condition for the molecular coalescence to be similar to two-quark coalescence is that the molecular size scales as $\sigma_F = \sigma_C T_C/T_F$, which is more or less satisfied by some exotic hadrons considered here, such as the $D_s(2317)$.

Our study also shows the interesting result that the ratio R_h^{CS} of the yield in the coalescence model to that in the statistical model is almost the same at RHIC and LHC. This similarity comes from the universal feature of the QCD phase transition; the common critical temperature and the common volume ratio V_C/V_H. In the nonrelativistic approximation shown in Eq. (3), it is possible to rewrite the statistical model yield in the coalescencelike form,

$$N_h^{\mathrm{stat}} = \frac{g_h V_H (m_h T_H)^{3/2}}{(2\pi)^{3/2}} e^{B/T_H} \prod_i \frac{N_{i,H}(2\pi)^{3/2}}{g_i V_H (m_i T_H)^{3/2}}, \quad (31)$$

where we consider the hadron h to be composed of several constituents, $B = \sum_i m_i - m_h$ is the binding energy, and $N_{i,H}$ represents the yield of the ith constituent at the volume V_H. This relation holds because the fugacity of a particle is equal to the product of the constituent fugacities, and the particle
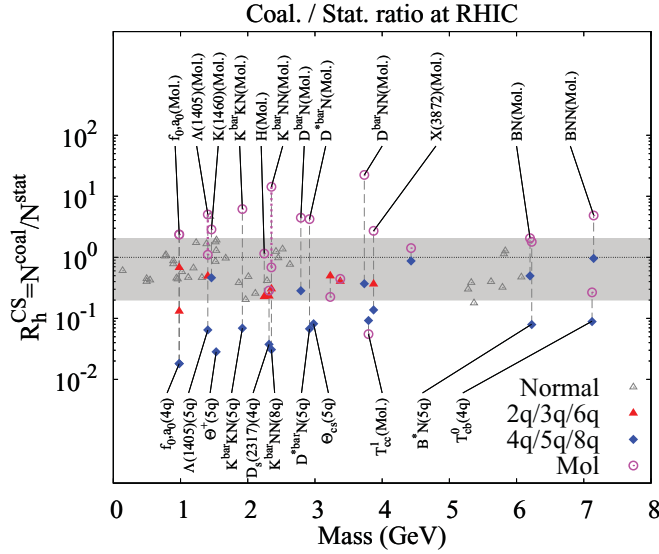
FIG. 2. (Color online) Ratio of hadron yields at RHIC in the coalescence model to those in the statistical model as a function of mass.

fugacity is related to the yield according to

$$\gamma_i = \frac{N_{i,H}}{g_h V_H} e^{m_h/T_H} \left(\frac{2\pi}{m_h T_H} \right)^{3/2}. \tag{32}$$

By using Eqs. (31) and (18), the ratio R_h^{CS} is found to be approximately given as

$$R_h^{\text{CS}} = e^{-\text{B}/T_H} \frac{M^{3/2} (2T_H/\omega)^{3(n-1)/2} (2T_c/\omega)^L}{m_h^{3/2} (1 + 2T_c/\omega)^{n-1+L}}$$

$$\times \frac{V_C}{V_H} \prod_i \frac{N_i/V_C}{N_{i,H}/V_H} \prod_{j=1}^{n-1} \frac{(2l_j)!!}{(2l_j+1)!!}. \tag{33}$$

Because T_C and T_H are the same at small baryon chemical potential, the particle density N_i/V_C, $N_{i,H}/V_H$ and the volume ratio V_C/V_H would be common at RHIC and LHC. As a result, the ratio of the production yield of hadrons in the coalescence model to that in the statistical model becomes the same at RHIC and LHC.

In Fig. 2, we show the hadron mass dependence of the ratio R_h^{CS} in heavy ion collisions at RHIC. The results are similar in heavy ion collisions at LHC as discussed in the above. It is seen that the effect of the internal structures of exotic hadrons on R_h^{CS} is particularly large for light exotic hadrons. We also show the ratio for normal hadrons. Here we have included the resonance decay contribution to pseudoscalar mesons such as $\rho \rightarrow 2\pi$ in evaluating the ratio. This estimate would be closer to the observational condition. As already mentioned, the ratios for normal hadrons are found to be in the range of $0.2–2$.

It should be noted that the coalescence model may overestimate the yield of very loosely bound molecules. Because the average hadron distance is around 2 fm and the temperature is $T_F = 125$ MeV at the thermal freeze-out, the loosely bound and spatially extended hadrons would dissociate easily through the final-state interactions with other hadrons. For example, the

deuteron yield is calculated to be around 1.4 per unit rapidity, which is larger than the statistical model prediction ($\sim$0.3). Experimental data seem to be consistent with the statistical model result, suggesting the possibility of later coalescence of loosely bound particles with a few MeV binding energies [134].

VI. SUMMARY

In this article, we have proposed a new approach of studying exotic hadrons in relativistic heavy ion collisions at RHIC and LHC. We have considered the yields of proposed exotic hadrons; $f_0(980)$, $a_0(980)$, $K(1460)$, $D_s(2317)$, T_{cc}^1, $X(3872)$, $Z^+(4430)$, and T_{cb}^0 for exotic mesons and $\Lambda(1405)$, $\Theta^+(1530)$, $\bar{K}KN$, $\bar{D}N$, $\bar{D}^*N$, Θ_{cs}, BN, and $\bar{B}^*N$ for exotic baryons, H, $\bar{K}NN$, $\Omega\Omega$, H_c^{++}, $\bar{D}NN$, and BNN for exotic dibaryons. To obtain the yields of these exotic multiquark hadrons or hadronic molecular states, we have used the coalescence model based on either the quark degrees of freedom or the hadronic degrees of freedom.

Our results indicate that the yields of many exotic hadrons are large enough to be measurable in experiments. In particular, heavy exotic hadrons containing charm and bottom quarks, as well as strange quarks, can be possibly observed at RHIC and especially at LHC. Therefore, relativistic heavy ion collisions will provide a good opportunity to search for exotic hadrons. In particular, it may lead to the first observation of new exotic hadrons. Also, we have found that the structure of light exotic hadrons has a significant effect on their yields in heavy ion collisions. For a hadron of normal quark structure, its production yield relative to the statistical model prediction $R_h = N_h/N_h^{\text{stat}}$ is found in the range of $0.2–2$. The yield ratio is smaller ($R_h < 0.2$) if a hadron has a compact multiquark configuration. For a hadron of molecular configuration with an extended size, its yield is, however, larger than the normal values ($R_h > 2$). Therefore, the ratios of measured yields from experiments on heavy ion collisions to those predicted by the statistical model provides a new method to discriminate the different pictures for the structures of exotic hadrons.

Our arguments here are mostly based on qualitative features of the yields. For example, we have regarded all hadrons to be stable in the hadronic phase and also neglected the effect of their widths on their production as well as the scattering effect on their strong decay products. As shown in Appendix C, the effect from the width of resonances is, however, small on exotic hadrons except for the light exotic hadron such as $f_0(980)$. So caution is required when we compare the production yields of $f_0(980)$ to the experimental data, and further study is needed for the yields of light exotic hadrons. Furthermore, we have assumed that all produced hadrons decouple instantaneously from the system without suffering final-state interactions. Although this effect is expected to play a minor role for some of the exotic hadrons because of their weak coupling to normal hadrons, as shown for $D_{sJ}(2317)$ in Ref. [19], more refined treatments of their dynamics in the hadronic phase, including their possible continuous decoupling from the system [135], are needed to obtain a more quantitative prediction of their yields. The improved study of exotic

hadrons in relativistic heavy ion collisions then will help answer longstanding problems on the existence and structure of exotic hadrons.

APPENDIX A: *d*-WAVE WIGNER FUNCTION

In this Appendix, we extend the calculation shown in Ref. [136] to construct the *d*-wave Wigner function from the harmonic oscillator wave functions. For this, we need the wave function of the second excited state, in addition to those of the ground and the first excited state, as the basis functions for the Wigner function,

$$
\begin{aligned}
\phi_0(x) &= \left(\frac{1}{b\sqrt{\pi}}\right)^{\frac{1}{2}} e^{-\frac{x^2}{2b^2}}, \\
\phi_1(x) &= \left(\frac{2}{b\sqrt{\pi}}\right)^{\frac{1}{2}} \frac{x}{b} e^{-\frac{x^2}{2b^2}}, \\
\phi_2(x) &= \left(\frac{1}{2b\sqrt{\pi}}\right)^{\frac{1}{2}} \left(2\frac{x^2}{b^2} - 1\right) e^{-\frac{x^2}{2b^2}},
\end{aligned}
\tag{A1}
$$

where $b^2 = \hbar/(m\omega)$. The *M*-state wave functions of the $L = 2$ state in Cartesian coordinates are then

$$
\begin{aligned}
\phi_{M=2}^{L=2}(\vec{r}) &= \frac{1}{2}[(\phi_2(x)\phi_0(y) - \phi_0(x)\phi_2(y)) \\
&\quad + i\sqrt{2}\phi_1(x)\phi_1(y)]\phi_0(z), \\
\phi_{M=1}^{L=2}(\vec{r}) &= \frac{1}{\sqrt{2}}(\phi_1(x)\phi_0(y) + i\phi_0(x)\phi_1(y))\phi_1(z),
\end{aligned}
$$

$$
\begin{aligned}
\phi_{M=0}^{L=2}(\vec{r}) &= \frac{1}{\sqrt{6}}(2\phi_0(x)\phi_0(y)\phi_2(z) \\
&\quad - \phi_2(x)\phi_0(y)\phi_0(z) - \phi_0(x)\phi_2(y)\phi_0(z)), \\
\phi_{M=-1}^{L=2}(\vec{r}) &= \phi_{M=1}^{L=2}(\vec{r})^*, \quad \phi_{M=-2}^{L=2}(\vec{r}) = \phi_{M=2}^{L=2}(\vec{r})^*.
\end{aligned}
\tag{A2}
$$

From the density matrix of the $L = 2$ state, which is defined by averaging over the *M* states,

$$
\begin{aligned}
\rho^{L=2}(\vec{r},\vec{r}') &= \frac{1}{5}\big[\phi_{M=2}^{L=2}(\vec{r})\phi_{M=2}^{L=2}(\vec{r}')^* + \phi_{M=1}^{L=2}(\vec{r})\phi_{M=1}^{L=2}(\vec{r}')^* \\
&\quad + \phi_{M=0}^{L=2}(\vec{r})\phi_{M=0}^{L=2}(\vec{r}')^* + \phi_{M=-1}^{L=2}(\vec{r})\phi_{M=-1}^{L=2}(\vec{r}')^* \\
&\quad + \phi_{M=-2}^{L=2}(\vec{r})\phi_{M=-2}^{L=2}(\vec{r}')^*\big],
\end{aligned}
\tag{A3}
$$

we obtain the *M*-averaged $L = 2$ harmonic oscillator Wigner function,

$$
\begin{aligned}
f^{L=2}(\vec{r},\vec{k}) &= \int \rho^{L=2}\left(\vec{r}+\frac{\vec{\eta}}{2}, \vec{r}-\frac{\vec{\eta}}{2}\right) e^{i\vec{k}\cdot\vec{\eta}} d\vec{\eta} \\
&= \frac{16}{30}\bigg[4\frac{r^4}{b^4} - 20\frac{r^2}{b^2} + 15 - 20b^2k^2 + 4b^4k^4 \\
&\quad + 16r^2k^2 - 8(\vec{r}\cdot\vec{k})^2\bigg] e^{-\frac{r^2}{b^2}-b^2k^2}.
\end{aligned}
\tag{A4}
$$

By replacing *b* with $\sigma(=1/\sqrt{\mu\omega})$, we obtain the *d*-wave coalescence factor using Eqs. (10) and (A4) as

$$
\frac{\int d^3y\, d^2k\, \tilde{f}(\vec{k}) f_d^W(\vec{y},\vec{k})}{\int d^3y\, d^2k\, \tilde{f}(\vec{k})} = \frac{(4\pi\sigma^2)^{\frac{3}{2}}}{V(1+2\mu T\sigma^2)^3} \frac{8}{15}(2\mu T\sigma^2)^2.
\tag{A5}
$$

APPENDIX B: COALESCENCE FACTOR FOR THE GENERAL MOMENTUM

We derive in this Appendix the coalescence factor for a general angular momentum *l* state given by Eq. (17). For constituents that are uniformly distributed in space, we can integrate the Wigner functions over space to obtain the momentum distribution of the constituents in the hadron. For the harmonic oscillator wave function of the lowest energy state with a given *l*, it is given by

$$
P_l(k) = (4\pi\sigma^2)^{3/2} \frac{(2\sigma^2 k^2)^l}{(2l+1)!!} e^{-\sigma^2 k^2},
\tag{B1}
$$

with the normalization $\int P_l(k)d^3k/(2\pi)^3 = 1$. The coalescence factor is then given by

$$
\begin{aligned}
F(\sigma,\mu,l,T) &= \int d^2k\, P_l(k) e^{-\frac{k^2}{2\mu T}} \bigg/ \int d^2k\, e^{-\frac{k^2}{2\mu T}} \\
&= \frac{(4\pi\sigma^2)^{3/2}}{1+2\mu T\sigma^2} \frac{(2l)!!}{(2l+1)!!} \left[\frac{2\mu T\sigma^2}{1+2\mu T\sigma^2}\right]^l.
\end{aligned}
\tag{B2}
$$

APPENDIX C: EFFECT OF FINITE WIDTHS OF RESONANCES ON HADRON YIELDS

In this Appendix, we briefly discuss the effects of the finite width from resonances on the production yields of exotic hadrons in both the statistical and the coalescence model.
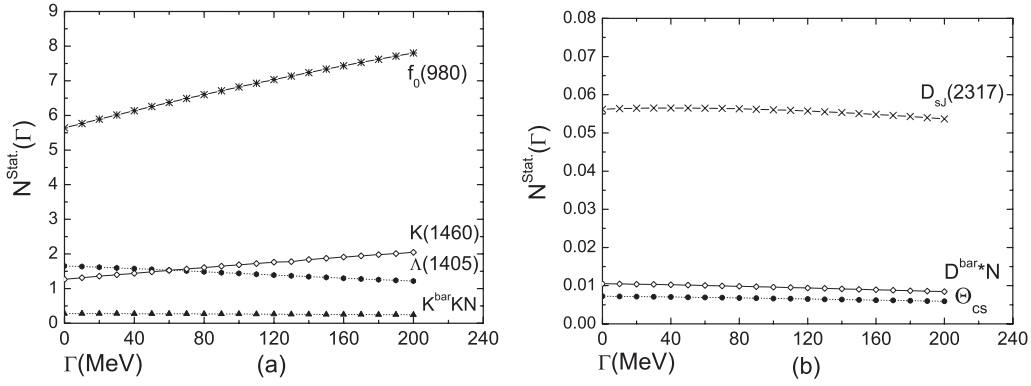
FIG. 3. Yields of selected exotic hadrons containing s (a) and c (b) quarks in the statistical model as functions of their width.

In the statistical model, the effect owing to the width of a particle on its yield can be included by adding in Eq. (1) an additional integration over the mass distribution of the particle. Taking the mass distribution to have a Breit-Wigner form with a peak mass m_h and a width Γ_h, Eq. (1) then becomes

$$N_{h,\Gamma_h}^{\text{stat}} = V_H \frac{g_h}{2\pi^2} \int_{M_{\text{th}}}^{\infty} \frac{dm}{N_{\text{BW}}} \int_0^{\infty} \frac{\Gamma_h}{(m - m_h)^2 + \Gamma_h^2/4}$$
$$\times \frac{p^2 dp}{\gamma_h^{-1} e^{\sqrt{m^2 + p^2}/T_H} \pm 1}, \quad \text{(C1)}$$

where M_{th} is the threshold for the dominant decay channel and N_{BW} is the normalization constant.

The exact information about the widths of exotic hadrons is, however, either not well determined or unavailable. For example, according to the Particle Data Group [44] the width of $f_0(980)$ is in the range between 40 and 100 MeV. Moreover, this broad range of the width can be related to a resonance spectral function and affect the yields of exotic hadrons such as $f_0(980)$, $a_0(980)$, $K(1460)$, $\Lambda(1405)$, $D_{sJ}(2317)$, $K\bar{K}N$, and charmed pentaquarks such as Θ_{cs} and $\bar{D}^*N$. To study the effect owing to the width of resonances on the yields of these exotic hadrons, we thus vary the width from 0 to 200 MeV in evaluating Eq. (C1). The resulting yields of above mentioned exotic hadrons are shown in Fig. 3 as functions of their widths. It is seen that the yields of these exotic hadrons in the statistical model do not change much except those of the light exotic hadrons such as $f_0(980)$ which increase by about 20% when its width is assumed to be 100 MeV and becomes closer to the estimated yield from the experimental data by STAR Collaboration [133].

The finite width of resonances can be similarly included in the coalescence model by folding the yield with the normalized mass distribution of a resonance. Because the yield of a hadron in the coalescence model does not depend on its mass, it is thus not affected by the additional integration over the mass distribution. However, the oscillator frequencies used in the hadron Wigner functions, which are determined from equating the yields obtained from the coalescence and the statistical models for normal hadrons, would be different once the width of resonances is included in the statistical model. As a result, the yields of exotic hadrons will be indirectly affected by the width of resonances. To study this effect, we recalculate the

oscillator frequency ω_s^{Γ} for the strange quark in the quark coalescence from Eq. (19) using the yields from the statistical model based on Eq. (C1), that is,

$$N_{\Lambda(1115),\Gamma}^{\text{stat,total}} = N_{\Lambda(1115)}^{\text{stat}} + \tfrac{1}{3} N_{\Sigma(1192)}^{\text{stat}} + N_{\Xi(1318)}^{\text{stat}}$$
$$+ \left(0.87 + \tfrac{0.11}{3}\right) N_{\Sigma(1385),\Gamma}^{\text{stat}}$$
$$+ N_{\Xi(1530),\Gamma}^{\text{stat}} + N_{\Omega^-(1672)}^{\text{stat}}$$
$$= 6.46 + \tfrac{1}{3} \times 13.57 + 4.73$$
$$+ \left(0.87 + \tfrac{0.11}{3}\right) \times 10.72 + 3.33 + 0.81$$
$$= 29.6. \quad \text{(C2)}$$

The major changes originate from the widths of $\Sigma(1385)$ and $\Xi(1530)$, which are $\Gamma_{\Sigma(1385)} = 37.1$ MeV and $\Gamma_{\Xi(1530)} = 9.5$ MeV according to the Particle Data Group [44] after averaging over the isospin of these resonances. To reproduce the total yield within the coalescence model with the constituent quark masses $m_{u,d} = 300$ MeV and $m_s = 500$ MeV, we need $\omega_s^{\Gamma} = 520.0$ MeV after taking into account the same feed-down contributions, and this differs from the previous value $\omega_s = 519$ MeV by only 1 MeV.

A similar consideration for the charm quark oscillator frequency ω_c^{Γ} based on the $\Lambda_c(2286)$ yield changes Eq. (21) to

$$N_{\Lambda_c(2286),\Gamma}^{\text{stat,total}} = N_{\Lambda_c(2286)}^{\text{stat}} + N_{\Sigma_c(2455),\Gamma}^{\text{stat}} + N_{\Sigma_c(2520),\Gamma}^{\text{stat}}$$
$$+ 0.67 \times N_{\Lambda_c(2625)}^{\text{stat}}$$
$$= 0.139 + 0.176 + 0.251 + 0.67 \times 0.048$$
$$= 0.598 \quad \text{(C3)}$$

after considering the widths of $\Gamma_{\Sigma_c(2455)} = 3.0$ MeV and $\Gamma_{\Sigma_c(2520)} = 16.0$ MeV. Fitting again the total yield of $\Lambda_c(2286)$ calculated in the statistical model to that in the coalescence model for the same resonances, we obtain $\omega_c^{\Gamma} = 386$ MeV for the charm quark mass $m_c = 1500$ MeV, compared with the value $\omega_c = 385$ MeV obtained previously without including the width of resonances. Because of the small differences between oscillator frequencies ω and ω^{Γ}, the production yields from the coalescence model given in Table V are essentially unchanged after the inclusion of the width of resonances.

[1] *Quark Matter 2009: Proceedings of the 21st International Conference on Ultrarelativistic Nucleus-Nucleus Collisions, Knoxville, Tennessee, 2009*, edited by P. Stankus, D. Silvermyr, S. Sorensen, and V. Greene (Elsevier, Amsterdam, 2009) [Nucl. Phys. A **830**, 1c (2009)].

[2] B. Aubert *et al.* (BABAR Collaboration), Phys. Rev. Lett. **90**, 242001 (2003).

[3] S. K. Choi *et al.* (Belle Collaboration), Phys. Rev. Lett. **91**, 262001 (2003).

[4] S. K. Choi *et al.* (BELLE Collaboration), Phys. Rev. Lett. **100**, 142001 (2008).

[5] For a recent review, see M. Nielsen, F. S. Navarra, and S. H. Lee, Phys. Rep. **497**, 41 (2010).

[6] N. Brambilla *et al.* (Quarkonium Working Group), *Heavy Quarkonium Physics, CERN 2005-005* (CERN, Geneva, 2005); N. Brambilla *et al.*, Eur. Phys. J. C **71**, 1534 (2011).

[7] R. L. Jaffe, Phys. Rev. D **15**, 267 (1977).

[8] R. L. Jaffe, Phys. Rev. D **15**, 281 (1977).

[9] R. L. Jaffe, Phys. Rev. Lett. **38**, 195 (1977); **38**, 617(E) (1977).

[10] R. H. Dalitz and S. F. Tuan, Ann. Phys. **10**, 307 (1960).

[11] N. Kaiser, P. B. Siegel, and W. Weise, Nucl. Phys. A **594**, 325 (1995).

[12] T. Hyodo and D. Jido, Prog. Part. Nucl. Phys. **67**, 55 (2012).

[13] T. Nakano *et al.* (LEPS Collaboration), Phys. Rev. Lett. **91**, 012002 (2003).

[14] S. H. Lee, S. Yasui, W. Liu, and C. M. Ko, Eur. Phys. J. C **54**, 259 (2008).

[15] S. H. Lee and S. Yasui, Eur. Phys. J. C **64**, 283 (2009).

[16] S. Yasui and K. Sudoh, Phys. Rev. D **80**, 034008 (2009).

[17] Y. Yamaguchi, S. Ohkoda, S. Yasui, and A. Hosaka, Phys. Rev. D **84**, 014032 (2011).

[18] L. W. Chen, V. Greco, C. M. Ko, S. H. Lee, and W. Liu, Phys. Lett. B **601**, 34 (2004).

[19] L. W. Chen, C. M. Ko, W. Liu, and M. Nielsen, Phys. Rev. C **76**, 014906 (2007).

[20] S. Cho *et al.* (ExHIC Collaboration), Phys. Rev. Lett. **106**, 212001 (2011).

[21] A. Ohnishi *et al.* (ExHIC Collaboration), AIP Conf. Proc. **1388**, 404 (2011).

[22] B. W. Zhang, C. M. Ko, and W. Liu, Phys. Rev. C **77**, 024901 (2008).

[23] R. C. Hwa and C. B. Yang, Phys. Rev. C **67**, 064902 (2003).

[24] V. Greco, C. M. Ko, and P. Levai, Phys. Rev. Lett. **90**, 202302 (2003); Phys. Rev. C **68**, 034904 (2003).

[25] R. J. Fries, B. Muller, C. Nonaka, and S. A. Bass, Phys. Rev. Lett. **90**, 202303 (2003); Phys. Rev. C **68**, 044902 (2003).

[26] A. Andronic, P. Braun-Munzinger, and J. Stachel, Nucl. Phys. A **772**, 167 (2006).

[27] K. Adcox *et al.* (PHENIX Collaboration), Phys. Rev. Lett. **88**, 242301 (2002).

[28] B. I. Abelev *et al.* (STAR Collaboration), Phys. Lett. B **655**, 104 (2007).

[29] S. S. Adler *et al.* (PHENIX Collaboration), Phys. Rev. Lett. **91**, 182301 (2003).

[30] P. Sorensen (STAR Collaboration), J. Phys. G **30**, S217 (2004).

[31] B. I. Abelev (STAR Collaboration), Science **328**, 58 (2010).

[32] Y. Kanada-En'yo and B. Muller, Phys. Rev. C **74**, 061901 (2006).

[33] B. I. Abelev *et al.* (STAR Collaboration), Phys. Rev. Lett. **97**, 132301 (2006).

[34] H. Sato and K. Yazaki, Phys. Lett. B **98**, 153 (1981).

[35] L. W. Chen, C. M. Ko, and B. A. Li, Phys. Rev. C **68**, 017601 (2003); Nucl. Phys. A **729**, 809 (2003).

[36] L. W. Chen and C. M. Ko, Phys. Rev. C **73**, 044903 (2006).

[37] Y. Oh, C. M. Ko, S. H. Lee, and S. Yasui, Phys. Rev. C **79**, 044905 (2009).

[38] S. H. Lee, K. Ohnishi, S. Yasui, I. K. Yoo, and C. M. Ko, Phys. Rev. Lett. **100**, 222301 (2008).

[39] Z. Y. Zhang, Y. W. Yu, C. R. Ching, T. H. Ho, and Z. D. Lu, Phys. Rev. C **61**, 065204 (2000).

[40] L. J. Reinders, H. Rubinstein, and S. Yazaki, Phys. Rept. **127**, 1 (1985).

[41] J. D. Weinstein and N. Isgur, Phys. Rev. D **41**, 2236 (1990).

[42] J. A. Oller and E. Oset, Phys. Rev. D **60**, 074023 (1999).

[43] M. G. Alford and R. L. Jaffe, Nucl. Phys. B **578**, 367 (2000).

[44] K. Nakamura *et al.* (Particle Data Group), J. Phys. G **37**, 075021 (2010).

[45] M. Albaladejo, J. A. Oller, and L. Roca, Phys. Rev. D **82**, 094019 (2010).

[46] A. M. Torres, D. Jido, and Y. Kanada-En'yo, Phys. Rev. C **83**, 065205 (2011).

[47] M. A. Nowak, M. Rho, and I. Zahed, Phys. Rev. D **48**, 4370 (1993).

[48] W. A. Bardeen and C. T. Hill, Phys. Rev. D **49**, 409 (1994).

[49] S. Godfrey and N. Isgur, Phys. Rev. D **32**, 189 (1985); S. Godfrey and R. Kokoski, *ibid.* **43**, 1679 (1991).

[50] Y.-B. Dai, C.-S. Huang, C. Liu, and S.-L. Zhu, Phys. Rev. D **68**, 114011 (2003).

[51] G. S. Bali, Phys. Rev. D **68**, 071501(R) (2003).

[52] A. Dougall, R. D. Kenway, C. M. Maynard, and C. Mc-Neile, Phys. Lett. B **569**, 41 (2003).

[53] A. Hayashigaki and K. Terasaki, arXiv:hep-ph/0411285.

[54] S. Narison, Phys. Lett. B **605**, 319 (2005).

[55] T. Barnes, F. E. Close, and H. J. Lipkin, Phys. Rev. D **68**, 054006 (2003).

[56] A. P. Szczepaniak, Phys. Lett. B **567**, 23 (2003).

[57] F. K. Guo, P. N. Shen, H. C. Chiang, R. G. Ping, and B. S. Zou, Phys. Lett. B **641**, 278 (2006).

[58] F. K. Guo, C. Hanhart, S. Krewald, and U. G. Meissner, Phys. Lett. B **666**, 251 (2008).

[59] F. K. Guo, C. Hanhart, and U. G. Meissner, Eur. Phys. J. A **40**, 171 (2009).

[60] E. E. Kolomeitsev and M. F. M. Lutz, Phys. Lett. B **582**, 39 (2004).

[61] J. Hofmann and M. F. M. Lutz, Nucl. Phys. A **733**, 142 (2004).

[62] E. van Beveren and G. Rupp, Phys. Rev. Lett. **91**, 012003 (2003).

[63] H.-Y. Cheng and W.-S. Hou, Phys. Lett. B **566**, 193 (2003).

[64] K. Terasaki, Phys. Rev. D **68**, 011501(R) (2003).

[65] L. Maiani, F. Piccinini, A. D. Polosa, and V. Riquer, Phys. Rev. D **71**, 014028 (2005).

[66] M. E. Bracco, A. Lozea, R. D. Matheus, F. S. Navarra, and M. Nielsen, Phys. Lett. B **624**, 217 (2005).

[67] T. Browder, S. Pakvasa, and A. A. Petrov, Phys. Lett. B **578**, 365 (2004).

[68] S. Zouzou, B. Silvestre-Brac, C. Gignoux, and J. M. Richard, Z. Phys. C **30**, 457 (1986).

[69] A. Selem and F. Wilczek, in *New Trends in HERA Physics 2005* (World Scientific, Singapore, 2006), pp. 337–356.

[70] J. Vijande, A. Valcarce and K. Tsushima, Phys. Rev. D **74**, 054018 (2006).

[71] A. V. Manohar and M. B. Wise, Nucl. Phys. B **399**, 17 (1993).

[72] J. Schaffner-Bielich and A. P. Vischer, Phys. Rev. D **57**, 4142 (1998).

[73] R. Chistov *et al.* (Belle Collaboration), Phys. Rev. Lett. **97**, 162001 (2006).

[74] K. Abe *et al.* (Belle Collaboration), Phys. Rev. Lett. **98**, 082001 (2007).

[75] P. del Amo Sanches *et al.* (BaBar Collaboration), Phys. Rev. D **82**, 011101 (2010).

[76] Yu. S. Kalashnikova and A. V. Nefediev, Phys. Rev. D **82**, 097502 (2010).

[77] T. J. Burns, F. Piccinini, A. D. Polosa, and C. Sabelli, Phys. Rev. D **82**, 074003 (2010).

[78] N. A. Tornqvist, Z. Phys. C **61**, 525 (1994).

[79] J. Hofmann and M. F. M. Lutz, Nucl. Phys. A **763**, 90 (2005).

[80] B. Aubert *et al.* (BaBar Collaboration), Phys. Rev. D **79**, 112001 (2009).

[81] R. Mizuk *et al.* (Belle Collaboration), Phys. Rev. D **80**, 031104(R) (2009).

[82] I. Adachi *et al.* (Belle Collaboration), arXiv:1105.4583 [hep-ex].

[83] E. Oset and A. Ramos, Nucl. Phys. A **635**, 99 (1998).

[84] J. A. Oller and U. G. Meissner, Phys. Lett. B **500**, 263 (2001).

[85] M. F. M. Lutz and E. E. Kolomeitsev, Nucl. Phys. A **700**, 193 (2002).

[86] D. Jido, J. A. Oller, E. Oset, A. Ramos, and U. G. Meissner, Nucl. Phys. A **725**, 181 (2003).

[87] T. Hyodo and W. Weise, Phys. Rev. C **77**, 035204 (2008).

[88] T. Hyodo, D. Jido, and A. Hosaka, Phys. Rev. C **78**, 025203 (2008).

[89] T. Sekihara, T. Hyodo, and D. Jido, Phys. Lett. B **669**, 133 (2008); Phys. Rev. C **83**, 055202 (2011).

[90] D. Diakonov, V. Petrov, and M. V. Polyakov, Z. Phys. A **359**, 305 (1997).

[91] C. Pinkenburg (PHENIX Collaboration), J. Phys. G **30**, S1201 (2004).

[92] R. De Vita *et al.* (CLAS Collaboration), Phys. Rev. D **74**, 032001 (2006).

[93] T. Nakano *et al.* (LEPS Collaboration), Phys. Rev. C **79**, 025210 (2009).

[94] A. Martinez Torres, E. Oset, Phys. Rev. Lett. **105**, 092001 (2010).

[95] A. Martinez Torres, E. Oset, Phys. Rev. C **81**, 055202 (2010).

[96] J. Randrup, Phys. Rev. C **68**, 031903 (2003).

[97] F. Becattini, M. Gazdzicki, A. Keranen, J. Manninen, and R. Stock, Phys. Rev. C **69**, 024905 (2004).

[98] J. Letessier, G. Torrieri, S. Steinke, and J. Rafelski, Phys. Rev. C **68**, 061901 (2003).

[99] R. L. Jaffe and F. Wilczek, Phys. Rev. Lett. **91**, 232003 (2003).

[100] A. Hosaka, M. Oka, and T. Shinozaki, Phys. Rev. D **71**, 074021 (2005).

[101] P. Gubler, D. Jido, T. Kojo, T. Nishikawa, and M. Oka, Phys. Rev. D **80**, 114030 (2009).

[102] D. Jido and Y. Kanada-En'yo, Phys. Rev. C **78**, 035203 (2008).

[103] A. Martinez Torres, K. P. Khemchandani and E. Oset, Phys. Rev. C **79**, 065207 (2009); A. Martinez Torres and D. Jido, *ibid.* **82**, 038202 (2010).

[104] D. O. Riska and N. N. Scoccola, Phys. Lett. B **299**, 338 (1993).

[105] A. Aktas *et al.* (H1 Collaboration), Phys. Lett. B **588**, 17 (2004).

[106] J. M. Link *et al.* (FOCUS Collaboration), Phys. Lett. B **622**, 229 (2005).

[107] H. J. Lipkin, Phys. Lett. B **195**, 484 (1987).

[108] C. Gignoux, B. Silvestre-Brac, and J. M. Richard, Phys. Lett. B **193**, 323 (1987).

[109] E. M. Aitala *et al.* (E791 Collaboration), Phys. Rev. Lett. **81**, 44 (1998).

[110] E. M. Aitala *et al.* (E791 Collaboration), Phys. Lett. B **448**, 303 (1999).

[111] K. Yamamoto *et al.* (E885 Collaboration), Phys. Lett. B **478**, 401 (2000).

[112] H. Takahashi *et al.*, Phys. Rev. Lett. **87**, 212502 (2001).

[113] M. Kobayashi and T. Maskawa, Prog. Theor. Phys. **44**, 1422 (1970); M. Kobayashi, H. Kondo, and T. Maskawa, *ibid.* **45**, 1955 (1971); G. 't Hooft, Phys. Rev. D **14**, 3432 (1976); **18**, 2199(E) (1978); Phys. Rep. **142**, 357 (1986).

[114] M. Oka and S. Takeuchi, Phys. Rev. Lett. **63**, 1780 (1989); Nucl. Phys. A **524**, 649 (1991).

[115] C. J. Yoon *et al.*, Phys. Rev. C **75**, 022201 (2007).

[116] A. Ohnishi, Y. Hirata, Y. Nara, S. Shinmura, and Y. Akaishi, Nucl. Phys. A **670**, 297c (2000); **691**, 242c (2001).

[117] T. Inoue *et al.* (HAL QCD collaboration), Prog. Theor. Phys. **124**, 591 (2010); Phys. Rev. Lett. **106**, 162002 (2011).

[118] S. R. Beane *et al.* (NPLQCD Collaboration), Phys. Rev. Lett. **106**, 162001 (2011)

[119] S. R. Beane *et al.* (NPLQCD Collaboration), Mod. Phys. Lett. A **26**, 2587 (2011).

[120] P. E. Shanahan, A. W. Thomas, and R. D. Young, Phys. Rev. Lett. **107**, 092004 (2011).

[121] Y. Akaishi and T. Yamazaki, Phys. Rev. C **65**, 044005 (2002).

[122] M. Agnello *et al.* (FINUDA Collaboration), Phys. Rev. Lett. **94**, 212303 (2005).

[123] V. K. Magas, E. Oset, A. Ramos, and H. Toki, Phys. Rev. C **74**, 025206 (2006).

[124] N. V. Shevchenko, A. Gal, and J. Mares, Phys. Rev. Lett. **98**, 082301 (2007).

[125] Y. Ikeda and T. Sato, Phys. Rev. C **76**, 035203 (2007).

[126] Y. Ikeda and T. Sato, Phys. Rev. C **79**, 035201 (2009).

[127] T. Yamazaki and Y. Akaishi, Phys. Rev. C **76**, 045201 (2007).

[128] A. Dote, T. Hyodo, and W. Weise, Nucl. Phys. A **804**, 197 (2008).

[129] A. Dote, T. Hyodo, and W. Weise, Phys. Rev. C **79**, 014003 (2009).

[130] Y. Ikeda, H. Kamano, and T. Sato, Prog. Theor. Phys. **124**, 533 (2010).

[131] S. Pal, C. M. Ko, and Z. Y. Zhang, Phys. Lett. B **624**, 210 (2005).

[132] C. Bignamini, B. Grinstein, F. Piccinini, A. D. Polosa, and C. Sabelli, Phys. Rev. Lett. **103**, 162001 (2009).

[133] P. Fachini (STAR Collaboration), Nucl. Phys. A **715**, 462 (2003).

[134] Y. Oh and C. M. Ko, Phys. Rev. C **76**, 054910 (2007).

[135] J. Knoll, Nucl. Phys. A **821**, 235 (2009).

[136] A. J. Baltz and C. Dover, Phys. Rev. C **53**, 362 (1996).